MAY 2020 M.Sc. in Aircraft and Aerospace Engineering AYKUT AKBULUT

REPUBLIC OF TURKEY

GAZİANTEP UNIVERSITY

GRADUATE SCHOOL OF NATURAL & APPLIED SCIENCES

ELECTRICAL EROSION MICRO HOLE DRILLING OF AEROSPACE MATERIALS

M.Sc. THESIS

IN

AIRCRAFT AND AEROSPACE ENGINEERING

BY

AYKUT AKBULUT

MAY 2020

ELECTRICAL EROSION MICRO HOLE DRILLING OF AEROSPACE MATERIALS

M.Sc. Thesis

in

Aircraft and Aerospace Engineering

Gaziantep University

Supervisor

Assoc. Prof. Dr. Kürşad GÖV

by

Aykut AKBULUT

May 2020

REPUBLIC OF TURKEY
GAZİANTEP UNIVERSITY
GRADUATE SCHOOL OF NATURAL & APPLIED SCIENCES
AIRCRAFT AND AEROSPACE ENGINEERING

Name of the Thesis : Electrical Erosion Micro Hole Drilling of Aerospace Materials

Name of the Student : Aykut AKBULUT

Exam Date : 22.05.2020

Approval of the Graduate School of Natural and Applied Sciences

Prof. Dr. A. Necmeddin YAZICI
Director

I certify that this thesis satisfies all the requirements as a thesis for the degree of Master of Science.

Assoc. Prof. Dr. İbrahim GÖV
Head of Department

This is to certify that we have read this thesis and that in our consensus opinion it is fully adequate, in scope and quality, as a thesis for the degree of Master of Science.

Assoc. Prof. Dr. Kürşad GÖV
Supervisor

Examining Committee Members:	Signature
Assoc. Prof. Dr. Bülent AKTAŞ (Chairman)	…………………..
Assoc. Prof. Dr. Eyüp YETER	…………………..
Assoc. Prof. Dr. Kürşad GÖV	…………………..

I hereby declare that all information in this document has been obtained and presented in accordance with academic rules and ethical conduct. I also declare that, as required by these rules and conduct, I have fully cited and referenced all material and results that are not original to this work.

Aykut AKBULUT

ABSTRACT

ELECTRICAL EROSION MICRO HOLE DRILLING OF AEROSPACE MATERIALS

AKBULUT, Aykut
M.Sc. in Aircraft and Aerospace Engineering
Supervisor: Assoc. Prof. Dr. Kürşad GÖV
May 2020
85 pages

High production standards are required in the aviation industry. One of these requirements is the dimentional accurancy and surface quality of the manufactured parts. Electrical Discharge Machining (EDM) is one of the precise production method in the non-traditional manufacturing methods. Micro hole-EDM is widely preferred for drilling high aspect ratio holes. In this study, Micro hole-EDM process was investigated and its effects on the aerospace materials were examined. These materials were selected as Nickel alloy Inconel 718 and Titanium alloy Ti-6Al-4V. The EDM parameters were selected as; discharge current (I), pulse on time (T_{on}) and pulse off time (T_{off}). The Output parameters were selected as; material removal rate (MRR), surface roughness value (R_a) and electrode wear rate (EWR). Design of Experiment (DOE) was created by the Taguchi method. The results were transformed into a mathematical model with regression analysis, and the relationship between input parameters and response parameters was interpreted through this model. Reliability of the model was analyzed by analysis of variance. With regression analysis optimization, it is aimed to reach the optimum values of MRR, EWR and R_a. Validity of the results was supported by validation experiments.

Key Words: Aerospace Materials, Electrical Discharge Hole Drilling, Electrical Discharge Machining, Titanium Alloy, Nickel Alloy

ÖZET

HAVACILIK MALZEMELERİNE ELEKTRİKSEL EROZYON İLE MİKRO DELİK DELİNMESİ

AKBULUT, Aykut
Yüksek Lisans Tezi, Uçak ve Uzay Mühendisliği
Danışman: Doç. Dr. Kürşad GÖV
Mayıs 2020
85 sayfa

Havacılık endüstrisinde yüksek üretim standartları gereklidir. Bu gereksinimlerden biri imal edilen parçalarının ölçü ve yüzey hassasiyetidir. Elektro Erezyonla İşleme (EEİ) geleneksel olmayan hassas üretim yöntemleri arasında önemli bir yere sahiptir. Mikro delik-EEİ, yüksek boy-çap oranına sahip delikleri delmek için yaygın olarak tercih edilir. Bu çalışmada, Mikro delik-EEİ süreci incelenmiş ve havacılık malzemeleri üzerine etkileri araştırılmıştır. Bu malzemeler Nikel alaşımı Inconel 718 ve Titanyum alaşımı Ti-6Al-4V olarak seçilmiştir. EEİ'nin etkilerini incelemek için giriş parametreleri olarak; deşarj akımı (I), akım uygulanma (T_{on}) ve bekletme (T_{off}) süresidir. Giriş parametrelerinin etkilerini analiz etmek için Çıktı parametreleri; malzeme kaldırma oranı (MKO), yüzey pürüzlülük değeri (R_a) ve elektrot aşınma oranıdır (EAO). Deney tasarımı (DT) Taguchi metodu ile oluşturulmuştur. Sonuçlar regresyon analizi ile matematiksel bir model haline getirilip, bu model aracılığıyla girdi parametreleri ve performans parametreleri arasındaki ilişki yorumlanmıştır. Modelin güvenilirliği varyans analizi ile doğrulanmıştır. Regresyon analizi optimizasyonu ile MKO, EAO ve R_a'nın optimum değerlerine ulaşılması hedeflenmiştir. Sonuçların geçerliliği validasyon deneyleri ile desteklenmiştir.

Anahtar Kelimeler: Havacılık Malzemeleri, Elektro Erezyon ile Delik Delme, Elektro Erezyonla İşleme, Titanyum Alaşım, Nikel Alaşım

''Dedicated to my family''

ACKNOWLEDGEMENTS

I owe my sincere thanks to my supervisor Assoc. Prof. Dr. Kürşad GÖV for their help, encouragement and precious information sharing during this thesis.

I also would like to express my sincere appreciation to all of my friends in university who helped me with physically and mentally.

Deepest gratitude is to my parents, who give me a real love, pray, support that all they have.

TABLE OF CONTENTS

Page

LIST OF TABLES

Page

LIST OF FIGURES

Page

LIST OF SYMBOLS

DOE	Design of Experiment
EDM	Electric Discharge Machining
WEDM	Wire Electric Discharge Machining
EWR	Electrode Wear Ratio
CFD	Computational Fluid Dynamics
MRR	Material Removal Rate
$\mathbf{R_a}$	Surface Roughness
SEM	Scanning Electron Microscope
$\mathbf{T_{on}}$	Pulse On Time
$\mathbf{T_{off}}$	Pulse Off Time
D	Diameter
I	Current
C	Capacitance
V	Voltage
Ti	Titanium Alloy (Ti-6Al-4V)
Ni	Nickel Alloy (Inconel 718)
Wt	Weight

CHAPTER I

INTRODUCTION

1.1 Introduction

Aircraft jet and gas turbine engines operate in harsh environments and manufacturers. These products must have high reliability performance under extreme conditions. Respond to these expectations, engine components made from super alloys. These materials have good mechanical and chemical properties as required. Such as high strength, high hardness, high melting point, low thermal conductivity and corrosion resistance. Inconel 718 and Ti-6Al-4V are common used and have a wide range of products in the aviation industry. Although they have high technical properties, they are difficult to shape and process. Traditional methods are inadequate. Some methods have developed to overcome these deficiencies. They are called as non-conventional methods. Electric Discharge Machining (EDM), Electric Chemical Treatment (ECM), Laser Treatment and Abrasive Water Jet Treatment are example of them. EDM is one of the most popular methods in the aviation industry. The extraordinary aspects of this method can be processed regardless of the mechanical and chemical properties of the material. EDM method can be used in materials with high melting point, high hardness and strength. The only negative side is that the material should be conductive.

1.2 Statement of the Problem

High aspect ratio holes are widely used in the industry. In addition, these holes contain some problems that need to be overcome. These problems arise as long drilling times, excessive material usage and the difficulty of machining with conventional manufacturing methods. Difficulties arise when applying to complex surfaces and hard material properties. Ventilation holes of metal molds, holes in turbine blades and medical components are examples of these products. These products have a high potential to observe such problems. These challenges can be overcome by using theEDM method in the industry. The functionality of the holes is related to the quality of production. Therefore, this study focuses on optimization of EDM parameter in high precision micro hole drilling.

1.3 Organization of the Thesis

This thesis starts with the introduction part about what the study is presented, the scope of the thesis and the aims to be achieved. The related literature is reviewed and discussed in the next section. In the third section, electric discharge machines are described. The fourth section covers the experimental setup and the procedure followed. The fourth section also provides details about the design of the experiments. These experiments describe how and which tools / equipment are used in these experiments. In the fifth section, modeling of EDM processes, experimental results and optimization results are presented. The sixth chapter contains the result.

CHAPTER II

LITERATURE SURVEY

2.1 Introduction

When processing methods are considered, different methods are encountered. These methods can be divided into traditional and non-traditional methods. Traditional methods include cutting, milling, drilling and similar machining methods. Non-traditional methods include electrical discharge machining, electrical chemical treatment, abrasive water-jet treatment and laser treatment. As a result, some inadequacy of traditional methods could consider. Cause of that, different processing methods were researched and non-traditional methods emerged. Nickel and Titanium alloys, which are frequently used in the aviation industry, are known as difficult to process. Due to the hardness of these materials, it is difficult to perform sensitive processes with conventional methods. At this point, EDM is preferred than the other methods. With EDM method, it is available to process irrespective to the strength, hardness and chemical properties of the material. The only negative side the EDM is that the material must be conducting electricity. Therefore, the development of EDM processing means increased mobility in the manufacturing field.

2.2 Literature Survey About EDM

Habib [1] examined the effects of EDM input parameters on surface quality, electrode wear rate, material wear rate and gap size as output parameters. It has formed a general mathematical model with the experimental data obtained from the experiments performed with EDM and compared these experimental results with the experimental results. To compare them, Response Surface Method was used and the reliability of the results were demonstrated by ANOVA. According to the results, optimum processing parameters of EDM were obtained.

Puranik [2] investigated the accuracy of high aspect ratio holes which were produced by using Micro-Electric Discharge Machining. In this study, it was concluded that the aspect ratio is higher than 25/1, when checking the process parameters. Experiments were designed with DOE. Processing parameters were electrode rotation, feed velocity, voltage, capacitance and resistance. The correctness of the test results were tested by ANOVA and 77% R^2 was obtained. The surface quality was observed and it was seen that affected by the debris. Statistical results were suggested that voltage is one of the most effective factors on hole accuracy.

Nihat *et al.* [3] studied on the effects of machining parameters and optimization of these parameters on the kerf (cutting width) and material removal rate in Wire Electrical Discharge Machining operations. In the article, experiments were performed within the scope of changing the parameters which were controlled from machine. Such as, pulse duration, open circuit voltage, wire speed and dielectric flushing pressure. Experiments were performed with Taguchi design to analyze the parameter's effects. These design results were used for modeled a mathematical formulation. This formula was created by using regression analysis method. Reliability of analysis results were inspected by ANOVA. The optimal machining parameters were selected to reach maximum MRR as well as the minimum kerf dimension by using established mathematical models.

Kumagai *et al.* [4] worked on a previously developed EDM system, which were used as a tool electrode with wire embedded in a dielectric tube and works as a jacket shown in Figure 2.1. The experimental parameters were determined as the optimum width of the current impulse, the optimum gap between the ends of the electrode with jacket and the optimum vibration amplitude of the electrode feed control. As a result, ~35% higher processing speed and ~40% less electrode wear were observed when compared with previous studies.

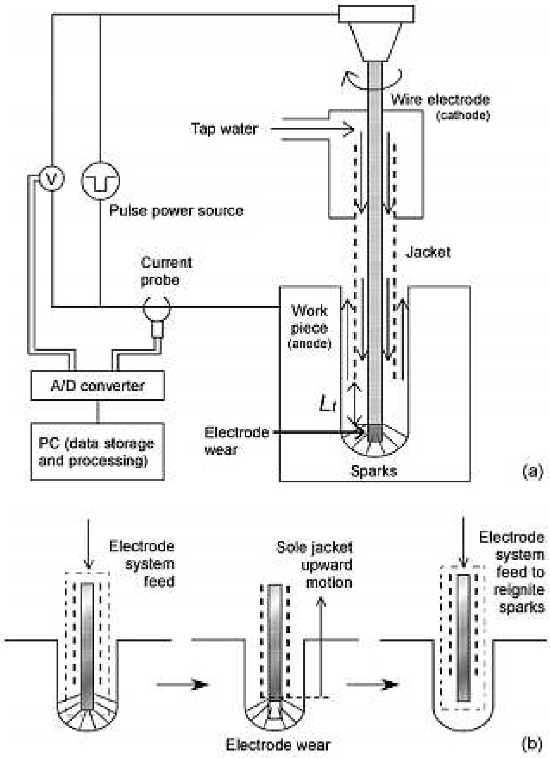

Figure 2.1 Assembly of the composite electrode EDM system: (a) system diagram and (b) electrode-motion diagram[4]

Debnath *et al.* [5], studied with using multiple regression analysis (MRA) and stated that the synergistic relationship of Electro Discharge Machining input and output parameter on the Al-4.5Cu-SiC composite. Machining parameters were selected as discharge current, pulse on time and pulse off time. The output parameters were chosen as metal removal rate (MRR), surface roughness (SR) and tool wear rate. In details, experiment results and MRA results were compared to understand the accessibility of results. Developed model results were occurred in the limits of the acceptable error and reached maximum error of 2.47% for metal removal rate (MRR), 0.621% for surface roughness (SR) and for tool wear rate (TWR). Results showed that MRA is suitable for minimum tool wear rate, minimum surface roughness and maximum material removal rate.

Meena and Azad [6], investigated the relation while Micro-Electric Discharge Machining (Micro-EDM) using on Ti-6Al-4V alloy with tungsten carbide electrode. As an input parameters current, voltage, frequency and width were chosen and as output parameters metal removal rate (MRR), tool wear rate (TWR) and overcut (OC) were chosen. Grey relational analysis and analysis of variance (ANOVA) was applied to optimize the levels of input parameters.

Eyercioglu *et al.* [7] studied on the investigating the influence of electro-discharge parameters on the surface integrity in small-hole drilling. To describe the effects of machine parameters, discharge current, pulse on time and pulse off time were chosen. Material removal rate, surface roughness, average white layer thickness, overcut and taper were taken as output parameters for this article. Workpieces were chosen as DIN 1.2080 (X210Cr12) cold working tool steel and machined with 2 mm single-hole brass electrodes. According to experiment results, dimensional precision increased during the machining and lower discharge currents (I\ 10A) were not sufficient to evaporate the molten material properly and result was low MRR (less than 0.06 g/min).

Bellotti *et al.* [8] studied on micro-EDM drilling, experiments were carried out to eliminate excessive wear of the electrode and unpredictable effects of process parameters. In these experiments, brass-tubular electrodes were used and micro-EDM effects on small holes for Ti-6Al-4V were observed. The experiments were designed with Taguchi experiment design and aimed the optimum settlement with using Gray relationship analysis. As machining parameters, material removal rate, tool wear rate and surface roughness were evaluated. As a result of the drilling processes, the tool breaks through were detected. The monitoring of the electrical signals can be used to effectively detect of breakthrough and prevent the machining surface located at the end of the hole.

Yilmaz *et al.* [9] studied that the creating an automated system for drilling hole with EDM on superalloys. Experiments were designed with design of experiment and were applied to Ti-6Al-4V and Inconel 718 alloys by drilling of different scale holes (0.4-3mm). The experiment results were filtered and analyzed using ANOVA to receive parameter relations and analytical modeling for optimization. ANFIS were chosen to correlate the EDM hole drilling parameters. They were chosen as pulse current, pulse duration/interval, capacitance, material removal rate, electrode wear and surface roughness. Results show that the promised system is a method that can be used for the production and repair of aero-engine parts to increase efficiency and increase sustainability.

Göv [10] investigated the influence of coolant on the performance of the Electro Discharge Hole Drilling process. To reach that, researcher performed the hole-EDM on die steel (DIN 1.2080) and used different types of cooling water such as distilled water, kerosene and water. All the other parameters were taken as constant and the response parameters were selected as processing speed, electrode wear, surface roughness (R_a) and white layer thickness. According to the results of the experiment, increasing the current was caused a decrease in the processing speed and increase white layer. Distilled water had relatively more reliable results than other types of coolants.

Liu *et al.* [11] investigated that the characteristic feature of edge disintegration easily appears on the electric discharge machining (EDM) drilling processing of cobalt-bonded tungsten carbide (WCCo). According to analyzing the experiments, response surface methodology (RSM) was applied. Experimental results that have 95% confidence interval, fairly well for the present the mathematical model of disintegration factor. The biggest effect on the disintegration were occurred by discharge current with capacitance value. The optimal settings of the process were obtained as reduction of the 5.53% disintegration factor.

Ekmekci *et al.* [12] worked on the geometry and surface damage which were produced by using micro electrical discharge machining. To better understand and figure out the cause of the undesired results, holes were machined with various pulse energies on plastic mold steel samples. The electrode was chosen as tungsten carbide. Micro-hole depth and over-cut were measured. Cracks were identified at some parts of hole which were occurred due to low pulse energy while machining applied.

Puri and Bhattacharyya [13] studied on modeling and analysis of white layer depth in a wire-cut EDM process. In this article, experiments were implemented with 4 variables and 5 levels. Experiments were described as mathematical model. Thanks to the model, the correlation between input parameters and responses were revealed. Pulse on time, wire tool offset and cutting speed were chosen as input parameters. The effects of process parameters on the white layer thickness were examined using the developed mathematical model.

Göv [14] investigated the effects of electrodes on the EDM hole drilling process with using different electrodes. These electrodes were made from single and multi channel brass and copper materials. Output parameters were chosen as machining speed, electrode wear ratio, surface roughness, and white layer thickness. Result shows, the single channel brass electrode had better machining speed and lower electrode wear compare to multi channel brass and copper electrodes.

Göv [15] investigated the effects of dissolved oxygen in the coolant liquid. For this, EDM drilling machine was used and DIN 1.2379 tool steel was used. Coolant which contain dissolved oxygen in different proportions were used. All processing parameters were kept constant. Effects of coolants were observed by recording response parameters. Such as processing speed, electrode wear rate, surface roughness, white layer thickness, and overcut diameter. The results were showed that it is possible to increase the processing speed by 20%, according to results. Within the results, the surface roughness were reduced from 4.5 to 2.4 μm.

Göv [16] studied the effects of dielectric fluid temperature on hole geometries which wer drilled by EDM. To find the effects on the response parameters, the workpiece has been selected as DIN 1.2379 tool steel and drilled with a single channel brass electrode. All processing parameters were kept constant, except for the temperature of the dielectric coolant. In order to understand the improvement in response parameters, the processing speed, electrode wear rate, surface roughness, white layer thickness and overcut in diameter were chosen. According to the results of the experiment, the material removal rate was increased by 30%. In addition, the white layer thickness was reduced by changing the temperature of the liquid.

Valaki *et al.* [17] studied on the technical feasibility of Jatropha curcas oil based bio dielectric fluid for electric discharge machining. The authors chose the response parameters as material removal rate, surface roughness and surface hardness. To investigate the quality of these parameters, current, gap voltage, pulse on time and pulse of time were chosen as input parameters. Results were analyzed with analysis of variance to show the reliability of the experiments. Results showed that the higher material removal rate, lower surface roughness occurred and the surface hardness were improved when oil based fluid was used compared to kerosene.

Fonseca and Marafona [18] observed the effect of deionization time on the electrical discharge machining performance. Parameters were selected as open voltage (gap width), current density, discharge duration and discharge interval. Performance parameters were chosen as the time needed for a complete deionization of the dielectric liquid, material removal rate and tool wear rate.

Ishida and Takeuchi [19] studied on the manufacturing of curved holes which were used generally in moulds. In accordance with this purpose, authors designed a simple mechanism which was occurred from combining different parts like spring, wire, pulleys and electrode for electrical discharge machining. The results showed that its enables to process curved line with this method.

Okada *et al.* [20] studied on the curved hole with electrical discharge machining like the previous article, but they worked with a suspended ball electrode by workpiece vibration as different. They were focused a curved hole on aluminum alloy and steel. The experiment results indicate that various types of curved holes were successfully drilled on the workpiece by EDM using the suspended ball electrode with workpiece vibration.

Maradia *et al.* [21] studied on the optimization of drilling operation with electrical discharge machining by using stochastic techniques. Within this purpose, an algorithm was designed for the electrical discharge machining process. Highest material removal rate was aimed with using different electrode lengths and shapes. After 40 iterations, the material removal rate was increased by 10 % at the end of the experiments.

Kumar and Parkash [22] investigated and optimized the electrical discharge machining input parameters. These parameters were selected as current, pulse on time, pulse off time and electrode material respectively. The response parameters were observed on the machining of aluminum boron carbide composite material. Taguchi was used to design of experiment and results were analyzed with analysis of variance. As a result, current was most effected parameters on the material removal rate and surface roughness. Electrode material was the most important parameter for electrode wear ratio.

Palanisamy *et al.* [23] studied on the experimental investigation and optimization of process parameters in EDM of aluminium metal matrix composites and input parameters were selected as discharge current, pulse on time and pulse off time respectively. To analyze the process effects on the material, response parameters were chosen as material removal rate, surface roughness and tool wear rate for alumina stir casted metal matrix composites. Design and optimize method was chosen as Grey relation analysis. The study revealed that the discharge current was the most effected parameter on the surface roughness and material removal rate.

Bellotti *et al.* [24] investigated the breakthrough phenomena in drilling micro holes by EDM. The authors were approached to the problem with analyzing the flushing mechanism of the debris particles affecting the discharging behavior while drilling process were applied. The amount of time which were spent in the breakthrough stage was proposed to reduce and results show that it was enabled to reduce the time by 60%.

Sapkal and Jagtap [25] optimized the micro EDM drilling process parameters on Titanium alloy. Copper-tungsten electrode was used to perform the experiments. Response surface methodology was used to design and analyze the experiments. Input parameters were chosen as pulse on time, discharge voltage, capacitance and electrode rotation speed and effects of these parameters observed on material removal rate, side gap width and taper ratio as response parameters. According to results, material removal rate was effected by discharge voltage, capacitance and electrode rotation speed.

Natsu and Maeda [26] studied on the realization of high-speed micro EDM for high-aspect-ratio micro hole with mist nozzle. The effectiveness of the mist nozzle was carried out to verify. When compared to the results of the mist jet and water jet, the effectiveness of the mist nozzle was approved.

Perveen and Jahan [27] studied on modeling and optimization of crater size generated during micro-EDM of Titanium alloy using response surface method. Experiments were applied as blind hole with 30 micron depth and were scanned with electron microscope. Crater size was selected as performance parameters and measured using

SEM image. Study results show that the response surface method was applied effectively to create a model to calculate the crater size.

Skrabalak [28] investigated the influence of electrode tool length on the micro EDM drilling performance. Experiments were performed with using steel samples which were drilled with variable electrode length. The main output parameters were chosen as tool wear ratio and material removal rate. Results were presented and discussed covered problems that came across during investigations.

Aharwal *et al.* [29] studied on the optimization of material removal rate and surface roughness in EDM machining of metal matrix composite using genetic algorithm. Workpiece was used as AlSiC and electrode was used as copper. Response parameters were chosen as material removal rate and surface roughness. Input parameters were chosen voltage, discharge current, pulse on time respectively. Optimization was implemented with using genetic algorithm. Results show that surface roughness was the best when material removal rate and current were low.

Kliuev *et al.* [30] investigated the flushing velocity and analysis during EDM drilling. The authors were aimed to increase flushing efficiency during erosion. Within this scope, dielectric flow trajectory was tracked by high speed imaging with an auxiliary magnification lens. Consequently, flushing efficiency was dropped by increasing of the drilling depth.

Dastagiri *et al.* [31] studied on the optimization of EDM process parameters by using heuristic approach. Experiments were studied with four input parameters as discharge current, pulse on time, discharge voltage and inter-electrode gap. All parameters were examined in three levels. Material removal rate, surface roughness and tool wear rate were selected as response parameters. The heuristic method has been adopted to predict the results.

Bhosle and Sharma [32] studied on multi-performance optimization of micro-EDM drilling process of Inconel 600 alloy. Gray relation analysis was used to develop a mathematical model. The material removal rate, taper angle, overcut and diameter variance of microhole were measured as performance characteristics. The most effected parameter on the taper angle was observed as capacitance. With this optimization, accuracy and surface quality of microholes were improved effectively.

Tripathy and Tripathy [33] investigated the surface characterization and multi-response optimization of EDM process parameters using powder mixed dielectric. Process parameters were chosen as powder concentration, peak current, pulse on time, duty cycle and gap voltage. Response parameters were chosen as material removal rate, surface roughness, recast layer thickness and micro-hardness respectively. Design of experiment was applied with Taguchi and L27 orthogonal array was selected to implement the experiments. Copper electrode were used to operate machining. Grey relational analysis was used to optimize the experiment results. As a result, improvement was figured out by 0.1055 grey relational grade and this result was occurred when the third level of parameters for powder concentration, first level of peak current, second level of pulse on time, third level of duty cycle and second level of gap voltage were used.

Begum and Reddy [34] investigated the effect of polarity on the machining characteristics and surface generation in EDM. Input parameters were chosen as pulse voltage, peak current, pulse on time and polarity respectively. The effect of input parameters were observed on the reponse parameters. They were chosen as surface finish and material removal rate.

Kumar *et al.* [35] studied on the modeling and optimization of hole circularity and hole dilation in electrical discharge drilling method. Experiments were implemented with using Taguchi design L27 orthogonal array. Input parameters were selected as discharge current, pulse on time, pulse of time and dielectric pressure. Analytic model was developed to optimize the experiment results and to do that Grey relation analysis was used. This analysis was allowed to minimize the uncertainty of the experimental data. Improvements figured out by 20% and 35% in hole circularity and hole dilation according to results.

Surya *et al.* [36] studied on the prediction of machining characteristics using artificial neural network in wire EDM of Al7075 based in-situ composite to achieve maximum material removal rate, minimum error on dimension and improvement on surface roughness. Input parameters were chosen as pulse on time, pulse off time, current and bed speed to analyze the experiments. An artificial neural network was developed with Taguchi L27 orthogonal array. According to results, developed model results were matched with experimental results sufficiently.

Jeykrishnan *et al.* [37] studied on optimization of process parameters in Electro-chemical machining (ECM) of D3 die steels. Experiments were designed with using Taguchi design. Workpiece material was chosen as D3 die steel. Input parameters were selected as current, voltage and electrolyte concentration. The effects of input parameters were observed within the scope of material removal rate and surface roughness. Current and electrolyte concentration were the most significant parameters that effected the surface roughness.

Mohanty *et al.* [38] researched an intelligent approach to optimize the EDM process parameters using utility concept and QPSO algorithm. In this research, different electrodes were used to compare their machinabilities like copper, graphite and brass. Workpiece material was selected as Inconel 718 superalloy. Experiments were designed with Taguchi and L27 orthogonal array implemented to obtain data for the study and analyzing. Output parameters were selected as material removal rate, tool wear rate, surface roughness and radial overcut. The other hand voltage, discharge current, pulse on time, duty factor, flushing pressure and electrode material were selected as input parameters. Optimal parameter settings were achieved by using both approaches according to results.

Rahul and Saurav [39] studied on electrical discharge machining of Inconel 825 using cryogenically treated copper electrode and compared with non-treated electrode. Surface cracks and white layers were investigated as well. Process parameters were selected as constant. Results indicated that white layer thickness thicker than non-treated electrode by ~26% which was obtained. Crack density was decreased relatively ~73% with cryogenically treated electrode against non-treated electrode.

Uhlmann *et al.* [40] investigated the comparative analysis of dry-EDM and conventional EDM for the manufacturing of micro holes in Si3N4-TiN. At this research, two different gases were used as dielectric (oxygen and argon) and conventional deionized water to manufacturing the micro holes. Experiments figured out that dry-EDM has higher effective pulse frequency and shorter relative motions between workpiece and tool electrode than the conventional EDM process.

Uhlmann *et al.* [41] studied on the electro-discharge drilling with MP-based carbon fibre electrodes. Carbon fibres were selected to drilling holes which are between 5 µm and 15 µm due to their good electrical conductivity. Experiments were implemented with non-rotating single carbon fibres as tool electrodes and the process parameters were optimized technically.

Risto *et al.* [42] investigated the optimization of the EDM drilling process to increase the productivity and geometrical accuracy. In this article, 2 mm diameter hole was aimed to produce precisely. According to this aim, four different electrodes were selected from 1.6 mm to 1.9 mm with 0.1 mm difference. Varying the input parameters setting, desired diameter was occurred.

Kliuev *et al.* [43] investigated that EDM drilling and shaping of cooling holes in Inconel 718 turbine blades. Authors were aimed to improve process capability and machining efficiency of aerospace alloys. Results were investigated within the scope of material removal rate, relative tool wear and surface integrity. According to results, material removal rate reached to 77 mm^3/min, relative tool wear was reduced down to 20% and recast layer thickness was reduced to 8 µm.

Antar *et al.* [44] compared two different drilling method capabilities. These methods were selected as high speed EDM and laser drilling. To understand the difference between two methods, 0.8 mm diameter hole was drilled on nickel based aerospace alloy. Results show that EDM has significantly better results in accordance with Laser drilling when focused on recast layer thickness and geometrical accuracy.

Fu *et al.* [45] investigated the surface roughness of piezoelectric self-adaptive Micro-EDM method. Using orthogonal experimental design and S/N analysis method, experiments were implemented. According to results, open voltage and capacitance were the most effective factors.

Lin *et al.* [46] studied on machining characteristics of a hybrid process of EDM in gas combined with ultrasonic vibration and abrasive jet machining. Machining characteristics were selected as material removal rate, electrode wear rate and surface roughness. Workpiece material was chosen as SKD 61 steel for all experiments. According to observations, hybrid EDM process has higher material removal rate. Oxygen was increased exploding and melting effects. Result of that highest material removal rate was occurred compared to air and argon.

Che *et al.* [47] studied on horizontal ultrasonic electrical discharge machining. In this article, a new ultrasonic method was developed which is worked on horizontal direction. Machining parameters were chosen as gap voltage, pulse interval, pulse width and peak current. According to results, traditional EDM worse than the new method by nearly 3 times about material removal rate and %20 worse than as regards processing accuracy.

Teimouri and Baseri [48] studied on the optimization of magnetic field assisted EDM using the continuous ACO algorithm. Two neuro-fuzzy inference system was designed and related with EDM parameters. Response parameters were chosen as material removal rate and surface roughness. Results of experiments which were implemented with ANFIS and continuous ant colony optimization were compared. Highest material removal rate and best surface quality were observed with CACO.

D'Urso and Merla [49] investigated that the workpiece and electrode influence on micro-EDM drilling performance. Authors were aimed to show the influence of different material combination effects on performance parameters. Workpiece materials were chosen four type stainless steel, titanium, magnesium and brass. Three type electrodes (copper, brass and tungsten carbide) were used also. The shape of electrode was chosen cylindrical and tubular respectively. Output parameters were chosen as tapereds and overcut. Tungsten carbide electrode was considered as the best in terms of tool wear, brass electrode was the worst performance about that.

Plaza *et al.* [50] investigated the experimental study on micro EDM-drilling of Ti-6Al-4V using helical electrode. The effects of input parameters effects were observed on the output parameters. These parameters were chosen as material removal rate, electrode rate, machining time and micro hole quality. Results show that machining time is reduced by 37% using 45° electrode.

2.3 Discussion

A literature search on EDM was conducted and result of the studies on the method were revealed. Titanium and Nickel alloys that are widely used in the aviation industry, there are inconsistencies in the size of these holes. In order to overcome these deficiencies, the study has been created. Input parameters should be associated with output parameters and input parameters should be optimized based on desired results. Also, the experiments usually consist of holes with a low aspect ratio. As a result, micro hole drilling should be done to better understand the process. In addition, improvement of machining parameters and reduction of processing time and high surface quality are also open to the development of hole quality parameters. For these purposes, a reliable mathematical model was needed.

CHAPTER III

BASIS OF ELECTRICAL DISCHARGE MACHINING

3.1 Introduction

In this chapter, different types of electrical discharge machines and their working principles are introduced. Main components of Ram-EDM machine, Fast-hole EDM machine, Wire EDM machine and their functions are given. The removal mechanism of EDM process is described and illustrated at Figure 3.1.

3.2 EDM Working Principles

It is the oldest technique that emerged as a mold sinking technology used among non-traditional production methods at the beginning of EDM history. This technology works by melting the material and removing the material from the processed material. Required heat energy is produced by electrical energy. Electricity flows between the electrode and the workpiece, the heat that causes the material to melt is released there, and the molten material is removed from the dielectric liquid.

The pressure of the dielectric fluid is an indirect factor that affects the process. While the molten material removing from the environment by high pressure liquid, a suitable environment is created to control the electric sparks. Low-pressure dielectric fluid is insufficient to remove molten material from the environment and can create an environment for a second discharge current. This effect complicates the control of the process. Another feature of the EDM method, the mechanical properties of the processed material have no effect on the process. Thermal properties such as melting point, boiling point and electrical conductivity are determining factors on the process.

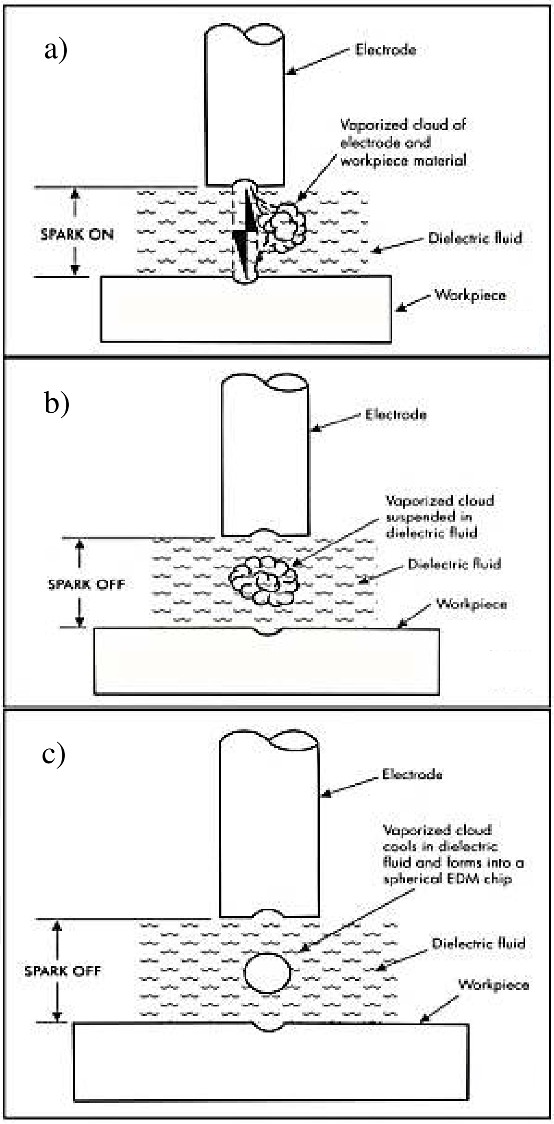

Figure 3.1 EDM working illustration a) Formation of vaporized cloud b) Vaporized cloud suspended in dielectric fluid c) Forming of debris [51]

3.3 Types of EDM

There are 3 types of applications in terms of EDM types. These are Ram/Sinker EDM, Fast-hole EDM and Wire EDM respectively. All of these machines works based on the same method. To remove the material from workpiece, uses sparks as thermal power [52]. However, different electrode types and dielectric fluids are used in different processing methods. Processing technology and their application areas are also different [53].

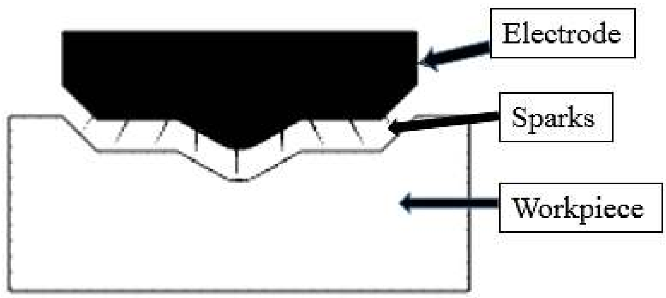

Figure 3.2 Ram type EDM [54]

Ram type EDM machines (Figure 3.1) are used to produce three-dimensional shapes by emptying the molds [51]. The electrode and workpiece are immersed in a dielectric liquid, usually hydrocarbon oil. A specially produced electrode is used to process the desired shape. In Ram EDM, spark occurs between opposing facing surfaces and the corners of the electrode and the workpiece. At the end of the process, the opposite shape of the electrode occurs on the workpiece.

Fast-hole EDM drilling machines have the same working principle as Ram EDM [52], as shown in Figure 3.2. High pressure dielectric fluid (deionized water) pumps into rotating hollow electrode. Rotating the electrode tube are main difference distinguished from other methods. This process can be used to produce fuel injectors, vent holes of injection molds, coolant holes of injection cutting tools, hardened staple ejector holes, wire-EDM start holes, holes in turbine blades and other similar holes.

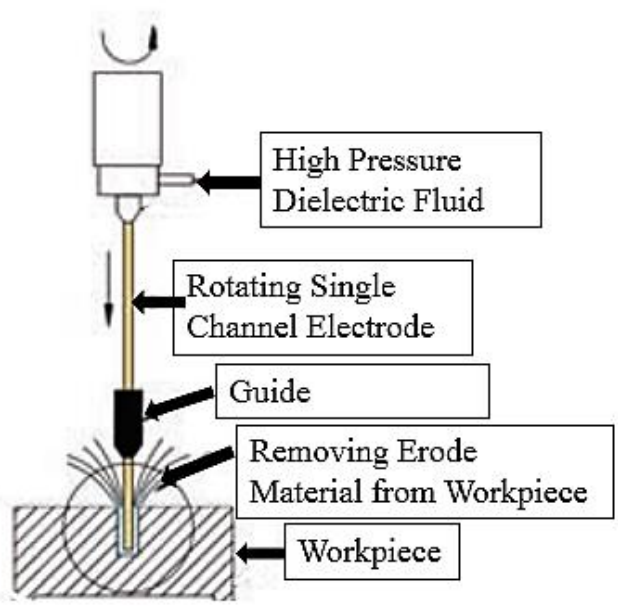

Figure 3.3 Fast-hole Drilling EDM Operation [53]

Wire EDM (Figure 3.3) is another form of EDM that uses a continuously moving electrode. The sparks occurs from the electrode wire surface to the workpiece. While the wire is being fed from reel to reel, material processing is realized by means of sparks. Desired path is formed by computer-controlled (CNC) movement of the machine[53]. The wire is usually made of brass or copper and the diameter varies from 0.1 to 0.3 mm. The dielectric fluid which are used in the wire EDM is generated to the processing surface.

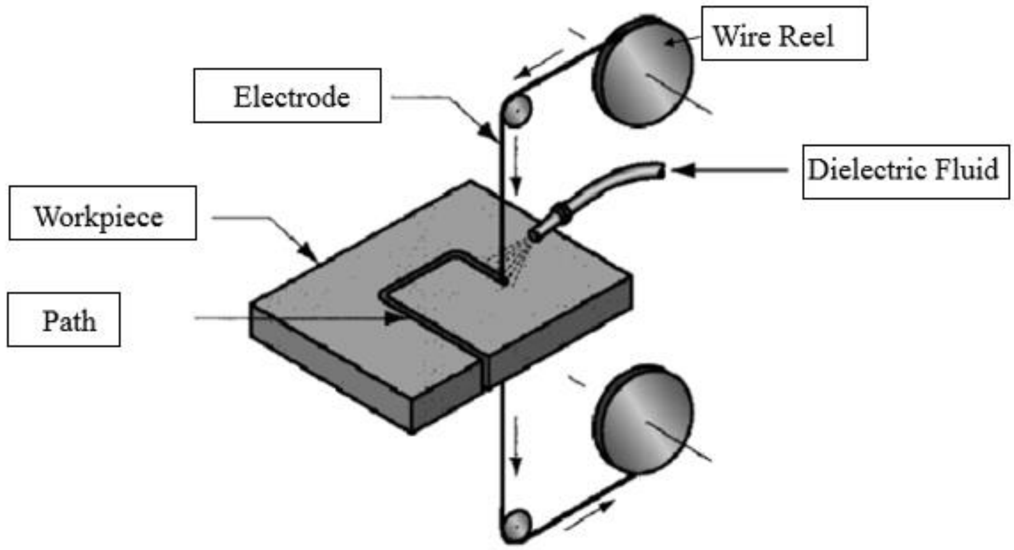

Figure 3.4 Wire EDM illustration [53]

CHAPTER IV

EXPERIMENTAL SETUP

4.1 Introduction

This section gives detail about the techniques, applied metods in the experiments and equipments. Statistical components were used to design the input parameters. Relation between input and output parameters were defined to estimate different parameter's result. In order to combine the experiment input parameters, DOE which is frequently used in the field, was used. The reliability of the experiment design was demonstrated by the analysis of variance.

The consistency of the results is questioned through validation experiments. Experiment design, application of the experiment, materials which were used and other equipment were discussed.

4.2 Electrical Discharge Machining Specifications

JS EDM AD-20 (Figure 4.1) type hole electrical discharge machine was used to perform the experiments which are available in Mechanical Engineering Department of Gaziantep University.

The machine allows to adjust the current intensity, voltage and frequency with control panel. In this study, discharge currents (I), pulse on time (T_{on}), pulse off time (T_{off}) were chosen as input parameters. It has been reported by previous research and these parameters the most effective electrical parameters [55-57]. Cavity voltage, electrode rotation, flushing pressure and polarity were taken as constant as shown in Table 4.1.

Table 4.1 Machining conditions

Discharge current (I)	3,4-8,8 A
Pulse on time (T_{on})	35-44 µs
Pulse off time (T_{off})	20-26 µs
Capacitance	104 µF
Voltage	30 V
Coolant liquid	deionized water
Dielectric flushing pressure	100 bar
Electrode rotation	200 rpm
Polarity of tool electrode	negative

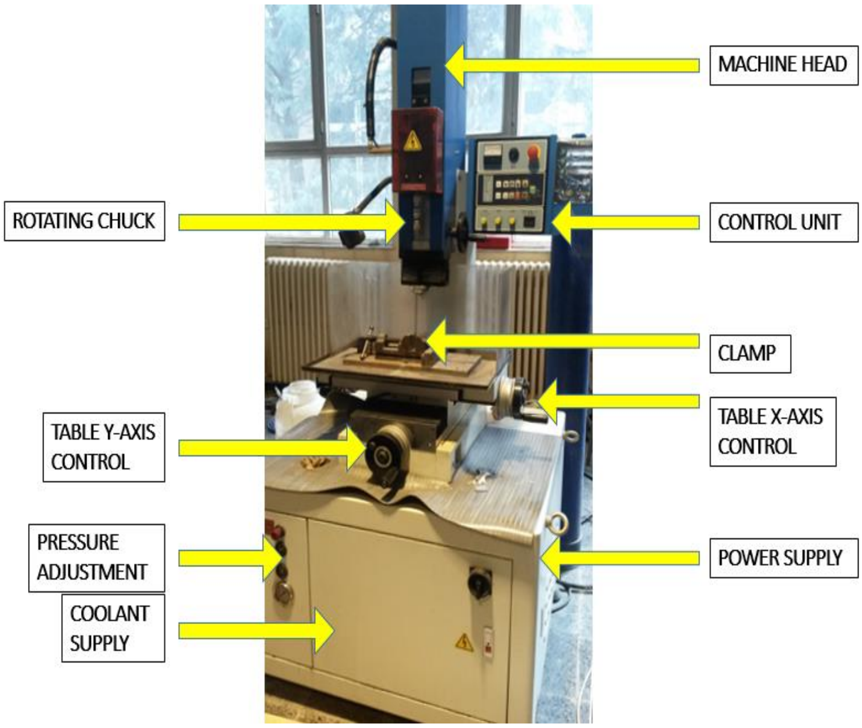

Figure 4.1 JS EDM AD-20 type Fast Hole EDM

4.3 Workpiece Material

The samples were chosen as Inconel 718 and Ti-6Al-4V (Table 4.2) due to their widespread application on aerospace and medical sectors. Workpieces were prepared as 5x10x20 mm blocks which were cut by Wire EDM (Figure 4.2). The faces which are opposite of each other, were ground by using 320 to 1000 size emery papers gradually and polished by using 1µm diamond suspension to investigate the result of tests. Also the properties of materials were shown in Table 3.3 for Inconel 718 and Table 3.4 for Ti-6Al-4V.

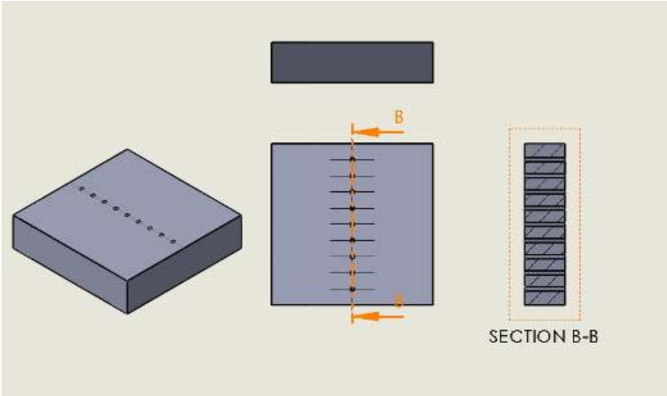

Figure 4.2 Workpiece illustration

Table 4.2 Chemical compositions of materials (wt. %)

	Ti-6Al-4V		
Ti	89,464	O	0,18
Al	6,08	C	0,02
V	4,02	N	0,01
Fe	0,22	H	0,0053
	Inconel 718		
Ni	52,5	Al	0,6
Cr	19	Si	0,35
Fe	17	Mn	0,35
Nb+Ta	5,125	Cu	0,3
Mo	3,05	C	0,08
Co	1	B	0,006
Ti	0,9		

Table 4.3 Properties of Inconel 718

Density	Kg/cu.m	8220
Electrical Resistivity	microhm-mm	1210
Melting point	°C	1210-1344
Modulus of elasticity	Gpa	208
Tensile Strength	Mpa	1407
%0.2 yield strength	Mpa	1172
Thermal conductivity	W/m-°K	11.4

Table 4.4 Properties of Ti-6Al-4V

Density	Kg/cu.m	4430
Electrical Resistivity	microhm-mm	1780
Melting point	°C	1604
Modulus of elasticity	Gpa	113.8
Tensile Strength	Mpa	950
%0.2 Yield strength	Mpa	880
Thermal conductivity	W/m-°K	7.2

4.4 Electrode Specification

Single channel electrodes with different sizes Ø300µm, 400µm and Ø500µm (Figure 4.3) were used to make holes on workpiece. The electrode properties were given in table 4.5. Various electrode materials can be used to drill holes with EDM. There are 3 types of material commonly used in general. One of the electrode type is made from copper and the other one is made from brass and the last one made from graphite. The different advantages and disadvantages of these three electrodes were observed in previous studies [58, 59]. The material of the electrode was selected by looking at some criteria. The size of the workpiece is determined according to the material properties and the type of EDM machine. In this study, brass electrode was used because of the following features. The main factors of choosing this material are high electrical conductivity and cheapness.

Figure 4.3 Ø500µm and Ø400µm electrodes

Table 4.5 Properties of electrode

Electrode Material	Brass
Melting point (°C)	900-940
Electrical resistivity (ohm-cm)	4.70
Thermal conductivity (W/m-°K)	159
Specific heat capacity (J/g-°C)	0.380
Channel type	single

4.5 Design of Experiment

Design of experiments (DOE) is an approach and used for decrease the number of experiments to accomplish the optimum conditions[60]. It is a statistical technique that made it possible to investigate not only the effect of factors but also their interactions. Statistical approaches are significant on planning, conducting, analyzing and interpreting the experimental data. The experimental design (DOE) allows to access the data to be obtained by testing all possibilities by doing less experiments. This saves both material and time. It is a statistical method that makes it possible to investigate their interactions with each other instead of just one parameter. Statistical approaches are very useful in planning, conducting and interpreting the experiments.

More than one method can be used for experimental design. As an example, Factorial design, response surface methodology (RSM), Taguchi, and Mixture design. The most common DOE technique is the Taguchi approach. Using the Taguchi approach, experimental design and analysis of results can be done with less effort and time. The Taguchi method uses a special orthogonal array design to examine the effects of the parameters in a small number of experiments [61]. Taguchi was applied using with statistical software, MINITAB®. Before performing the experiments, the cause of identifying the suitable machine parameters, preliminary experiments were investigated and reached the results which mostly effected on response parameters were I, T_{on}, T_{off} respectively [62]. Fast-hole EDM machine has ten level settings as 0 to 9 for all input parameters. According to preliminary experiments, level of parameters from 0 to 4 had no substantial effects on response parameters [62]. In other words, under the set of 4, there is no exist suitable hole on the workpiece. So, there is no data to inspect and analyze for better MRR, EWR and R_a. Result of that, in this experiment, machine parameters have been set from four to six for current and six to nine for pulse on time and pulse off time.

In this study, three L9 orthogonal array (OA) designs were used to examine the experiments. Each set was designed according to electrode diameter. Each test group has 3 factors (I, T_{on}, T_{off}) and three levels (Table 4.6). Parameter values were combined according to the L9 test setup were shown in Table 4.7.

Table 4.6 Machining parameters

Levels	A I (ampere)	B T_{on} (μs)	C T_{off} (μs)
1	3,4	35	20
2	8,2	38	23
3	8,8	44	26

Table 4.7 L9 Taguchi experiment design

Experiment no	L9 Taguchi Design			Machine Parameters			Parameter Values		
	A	B	C	I	T_{on}	T_{off}	I(A)	T_{on}(μs)	T_{off}(μs)
1	1	1	1	4	7	7	3,4	35	20
2	1	2	2	4	8	8	3,4	38	23
3	1	3	3	4	9	9	3,4	44	26
4	2	1	2	5	7	8	8,2	35	23
5	2	2	3	5	8	9	8,2	38	26
6	2	3	1	5	9	7	8,2	44	20
7	3	1	3	6	7	9	8,8	35	26
8	3	2	1	6	8	7	8,8	38	20
9	3	3	2	6	9	8	8,8	44	23

4.6 Experimental Procedure

In this experiment, studies focused on two different materials commonly used in aerospace industry. One of them is Inconel 718 and the other one is Ti-6Al-4V. Both of them have different mechanical properties and they are nickel and titanium alloys. Both have good thermal and physical properties in spite of poor machinability that why widely used aerospace industry. In order to drill these workpieces, single channel brass electrode were selected. This material is commonly used in the EDM process, especially aerospace alloys [63, 64]. The dimension of hole diameters has a wide range which were expected from the industry. Generally, these holes were limited between

0.2 to 3mm diameters. These diameter values are penetrable with EDM Fast-hole drilling machine. That is available with this machine to reach the Ø50µm holes actually. This study focused on micro hole drilling operations. To do that Ø300-400-500µm electrodes were used on each types material (Figure 4.4). It is hard to drill with smaller dimensions as demonstrated with previous researches. Generally, a problem occurred and electrodes were cut-off during drilling operations [62].

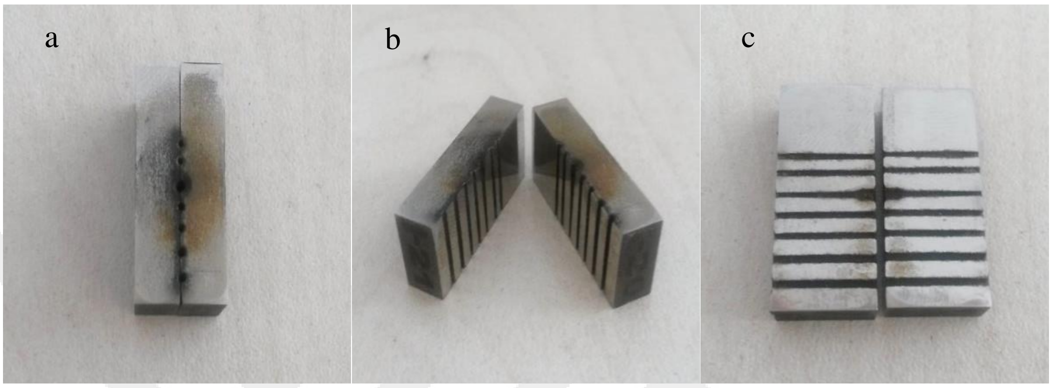

Figure 4.4 (a)Top view of workpiece, (b)Half-open view of workpiece and (c)Inside of workpiece

4.7 Experimental Measurements

4.7.1 Material Removal Rate (MRR)

Workpieces were weighed to calculate the material removal rate. The workpieces were weighed twice, before and after drilling, and each part of the workpiece weight recorded separately. The values were calculated to figure out how much weight lose. Weight changes per minute were calculated to understand the effect of the parameters on the material removal rate (Equation 4.1). All weight measurements were made with the SHIMADZU AUX220 (Figure 4.5) and an electronic timer was used to measure drilling takes how much time.

$$\text{MRR}\left(\frac{\text{mg}}{\text{min}}\right) = \frac{\text{Initial weight of material - final weight of material}}{\text{Machining Time}} \tag{4.1}$$

Figure 4.5 SHIMADZU AUX220 Balance

4.7.2 Electrode Wear Ratio (EWR)

During the EDM process, sparks occurs at the electrode head and reaches high temperatures. These sparks melt the surface of the workpiece and remove the molten material with pressurized water. While this process, electrode melts and the small parts break off from the tip of the electrode. This is called electrode wear, which directly affects the EDM process performance. Electrode wear adversely affects EDM performance. The lower the electrode wear rate means better. Therefore, electrode weights were checked before and after the operation. To calculate EWR, datas were obtained as shown in Equation 4.2.

$$\mathrm{EWR}\left(\frac{\mathrm{mg}}{\mathrm{min}}\right)=\frac{\text{Initial weight of electrode - final weight of electrode}}{\text{Machining Time}} \tag{4.2}$$

4.7.3 Surface Roughness (R_a)

Depending on the operating conditions, different types of fluids may pass through the formed holes. Each fluid are affected by the roughness of the surface. At this point, the surface roughness should be kept minimum if the flow is desired to be smooth.

Minimizing surface roughness, air, fuel, etc. It has a positive effect on the physical properties. Machine parameters have a direct effect on surface roughness. Surfaces that formed result of the experiments were recorded with Mitutoyo SJ 401 stylus surface roughness measuring device. Measured surface length was selected as 4 mm and all measurements were made by re-measuring 3 times as shown in Figure 4.6.

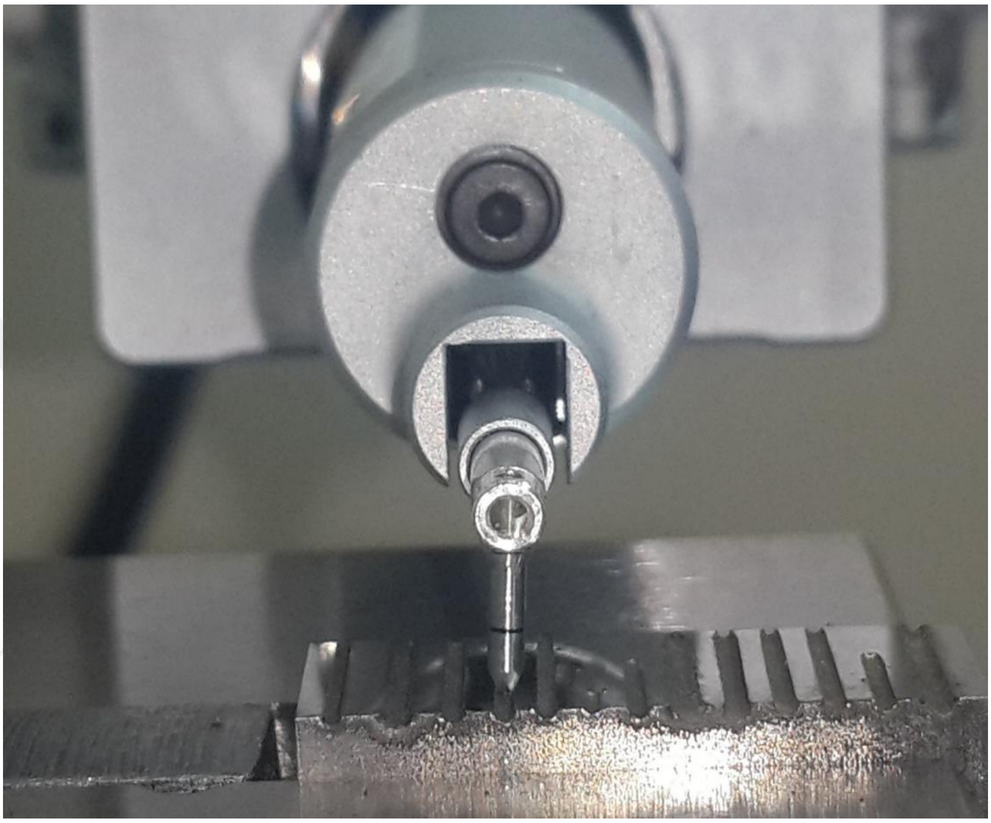

Figure 4.6 Example of surface roughness measurement

CHAPTER V

MODELING AND OPTIMIZATION OF THE EDM FAST HOLE DRILLING OPERATIONS

5.1 Experimental Results of EDM Fast Hole Drilling Operations

According to experiment inspections, the datas which were obtained from the measurements, shown from the Table 5.1 to Table 5.6 respectively. All tables shows the measurement of MRR, EWR and R_a values for each different electrode dimensions. Hole dimensions are Ø500-400-300µm separately. Also, SEM images were shown in Figure 5.1 to Figure 5.6 respectively for each different material and dimension.

Table 5.1 Measurements of MRR, EWR, R_a / Ti-6Al-4V / Ø500µm

Ti-6Al-4V Ø500µm						
experiment no:	Machine Parameters			MRR (mg/min)	EWR (mg/min)	R_a (µm)
	I (A)	T_{on} (µs)	T_{off} (µs)			
1	3,4	35	20	3,8076	0,6380	16,71
2	3,4	38	23	3,4216	0,4526	13,18
3	3,4	44	26	2,2888	0,4087	14,64
4	8,2	35	23	11,2767	3,9092	5,15
5	8,2	38	26	9,9750	3,5461	8,51
6	8,2	44	20	12,4678	4,7595	7,95
7	8,8	35	26	13,0151	4,2516	4,69
8	8,8	38	20	11,1337	4,8805	5,22
9	8,8	44	23	12,5470	5,7610	5,81

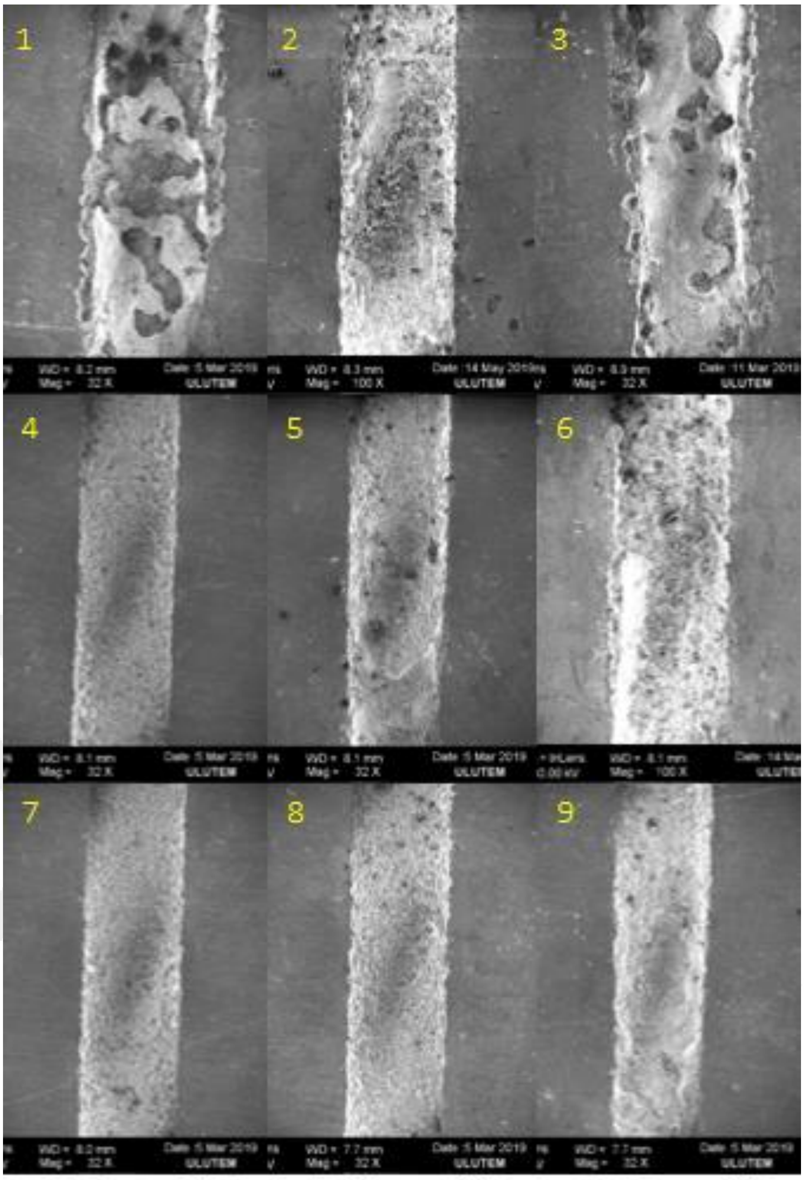

Figure 5.1 Ti-6Al-4V Ø500µm Hole drilling experiment's SEM images

Table 5.2 Measurements of MRR, EWR, R_a / Ti-6Al-4V / Ø400µm

Ti-6Al-4V Ø400µm						
experiment no:	Machine Parameters			MRR (mg/min)	EWR (mg/min)	R_a (µm)
	I (A)	T_{on} (µs)	T_{off} (µs)			
1	3,4	35	20	1,7129	0,4107	13,24
2	3,4	38	23	2,4950	1,1570	18,41
3	3,4	44	26	1,1677	0,6400	16,68
4	8,2	35	23	4,8721	2,1437	15,53
5	8,2	38	26	5,7200	3,5610	9,68
6	8,2	44	20	3,1000	2,1500	11,61
7	8,8	35	26	7,2599	3,4979	6,69
8	8,8	38	20	8,4473	3,8684	7,90
9	8,8	44	23	7,9810	3,7090	7,01

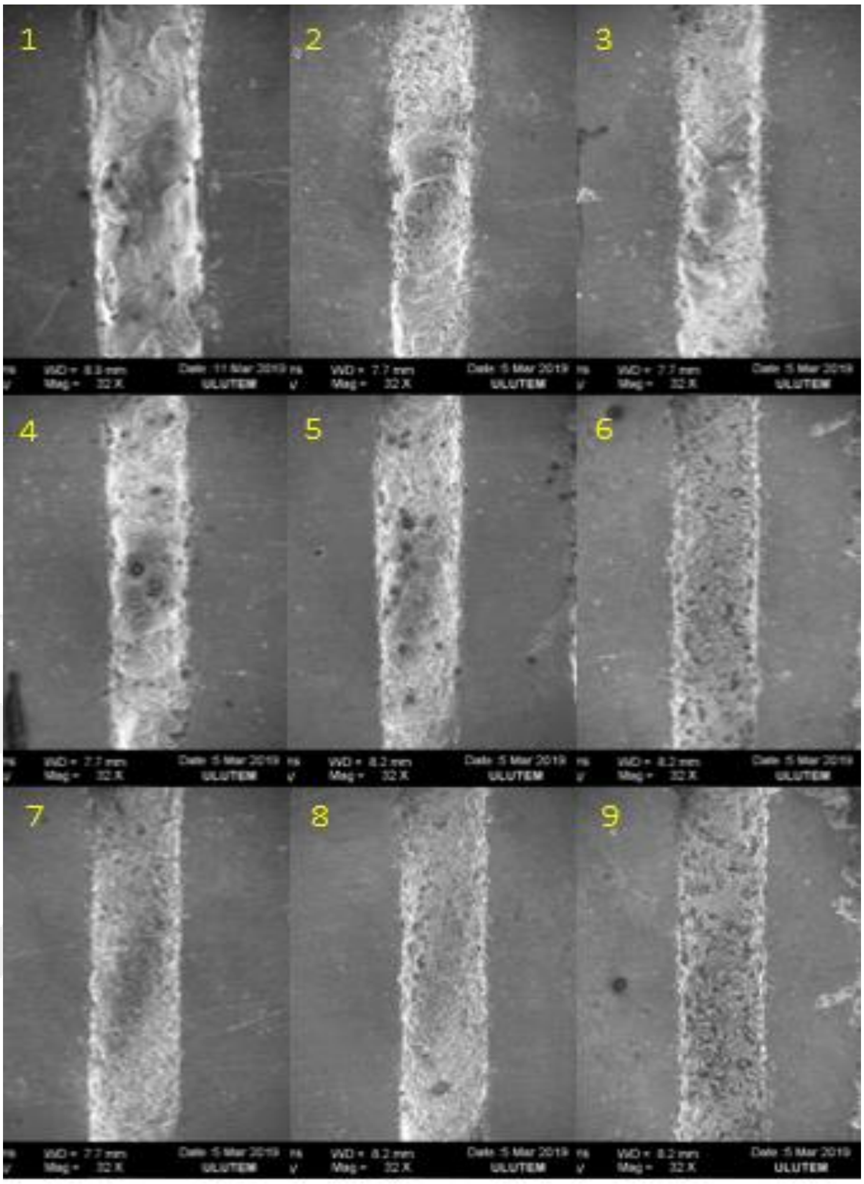

Figure 5.2 Ti-6Al-4V Ø400µm Hole drilling experiment's SEM images

Table 5.3 Measurements of MRR, EWR, R_a / Ti-6Al-4V / Ø300µm

Ti-6Al-4V Ø300µm						
experiment no:	Machine Parameters			MRR (mg/min)	EWR (mg/min)	R_a (µm)
	I (A)	T_{on} (µs)	T_{off} (µs)			
1	3,4	35	20	0,9849	2,2226	22,69
2	3,4	38	23	1,2000	2,3620	18,35
3	3,4	44	26	0,9980	2,1251	20,93
4	8,2	35	23	3,7500	3,8400	10,19
5	8,2	38	26	4,1900	3,3460	7,26
6	8,2	44	20	4,3202	2,7530	7,07
7	8,8	35	26	3,9145	1,8447	8,99
8	8,8	38	20	4,0260	2,3006	10,76
9	8,8	44	23	4,1800	2,0110	9,23

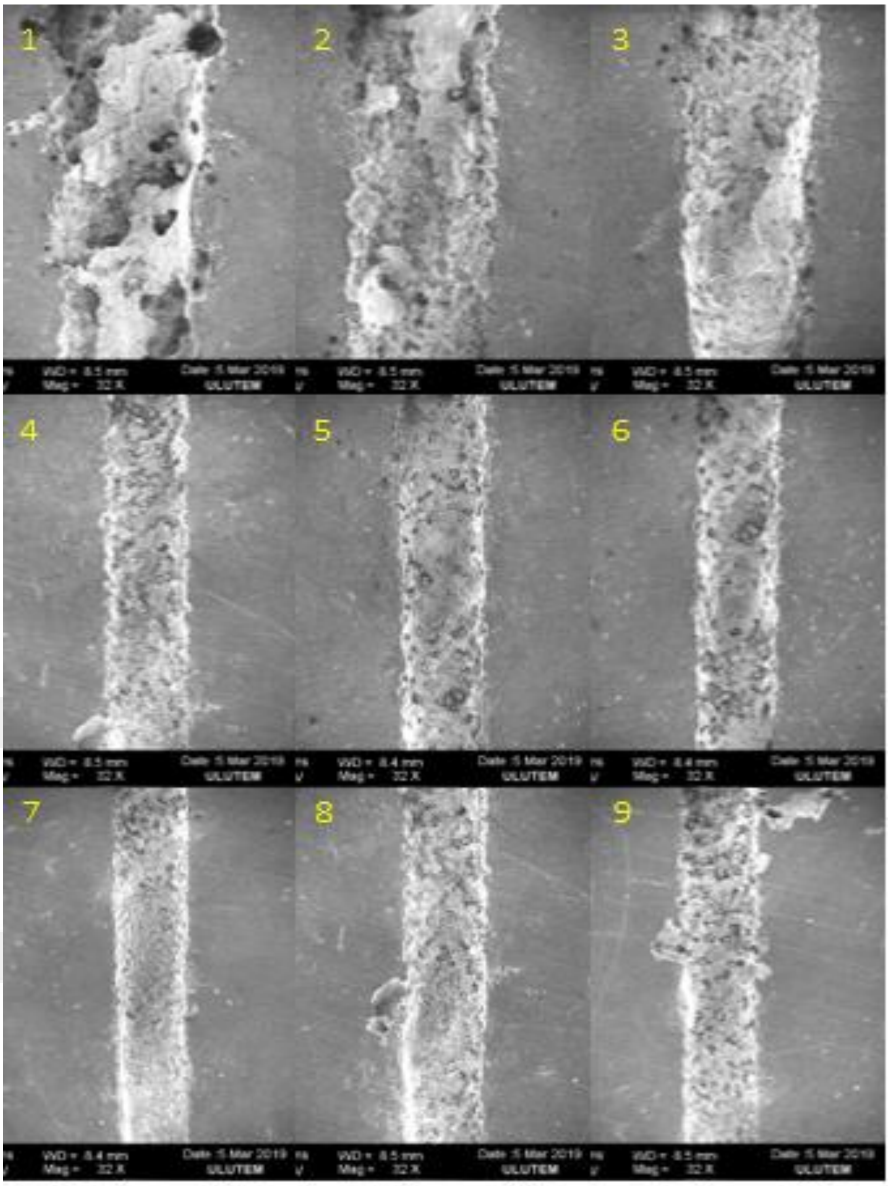

Figure 5.3 Ti-6Al-4V Ø300µm Hole drilling experiment's SEM images

Table 5.4 Measurements of MRR, EWR, R_a / Inconel 718 / Ø500µm

Inconel 718 Ø500µm						
experiment no:	Machine Parameters			MRR (mg/min)	EWR (mg/min)	R_a (µm)
	I (A)	T_{on} (µs)	T_{off} (µs)			
1	3,4	35	20	14,2200	4,1609	6,01
2	3,4	38	23	13,6100	3,6658	10,78
3	3,4	44	26	11,1945	2,0421	8,95
4	8,2	35	23	23,3552	6,3761	8,38
5	8,2	38	26	21,7861	5,9260	9,12
6	8,2	44	20	16,1920	5,3310	6,71
7	8,8	35	26	23,8486	7,7224	3,43
8	8,8	38	20	17,1244	5,2887	3,21
9	8,8	44	23	15,2152	4,5338	3,49

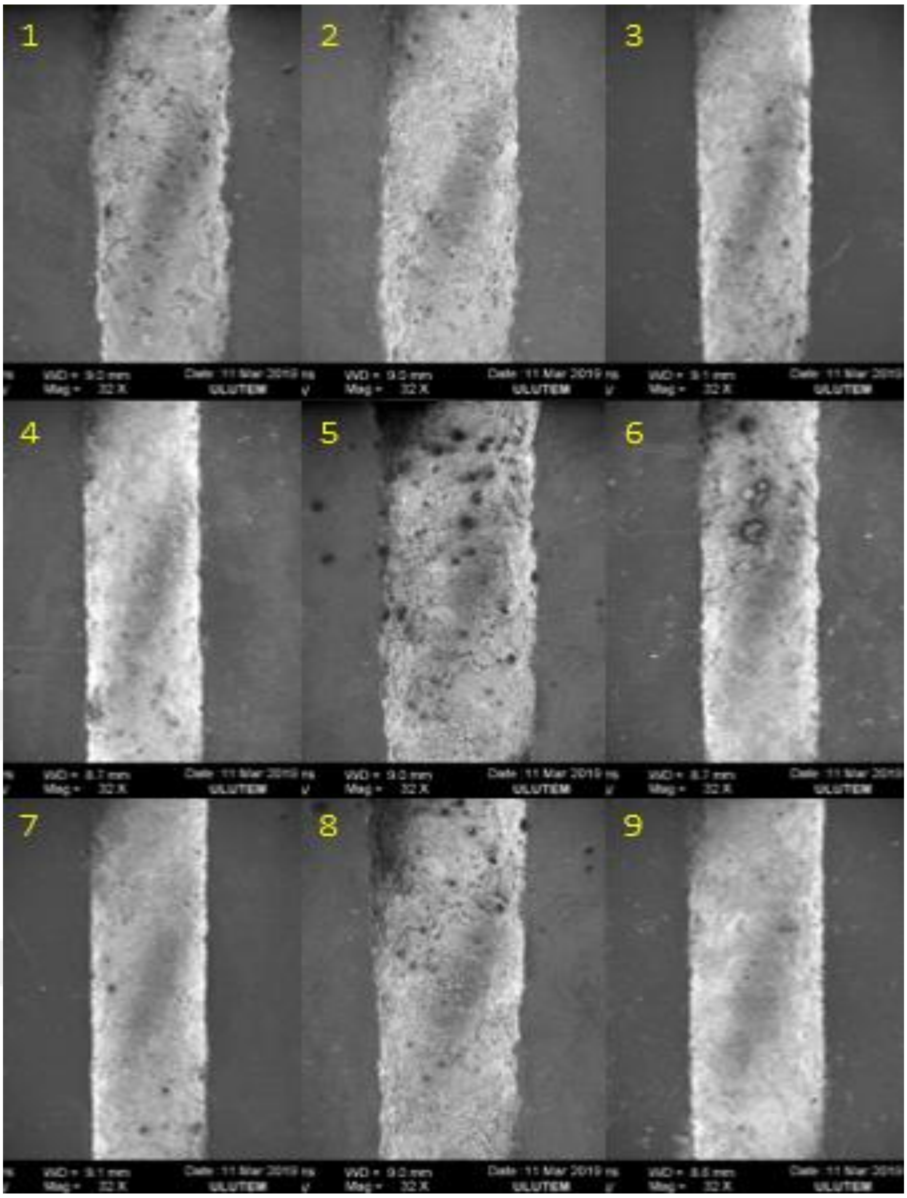

Figure 5.4 Inconel 718 Ø500μm Hole drilling experiment's SEM images

Table 5.5 Measurements of MRR, EWR, R_a / Inconel 718 / Ø400μm

Inconel 718 Ø400μm						
experiment no:	Machine Parameters			MRR (mg/min)	EWR (mg/min)	R_a (μm)
	I (A)	T_{on} (μs)	T_{off} (μs)			
1	3,4	35	20	5,7260	0,6292	8,19
2	3,4	38	23	3,9860	1,1766	5,4
3	3,4	44	26	3,5688	0,9843	7,67
4	8,2	35	23	12,0902	2,1110	5,57
5	8,2	38	26	10,8990	3,4652	3,85
6	8,2	44	20	9,7410	3,6231	3,51
7	8,8	35	26	13,9992	4,5274	3,53
8	8,8	38	20	13,6540	4,6521	2,95
9	8,8	44	23	10,2452	3,1583	2,32

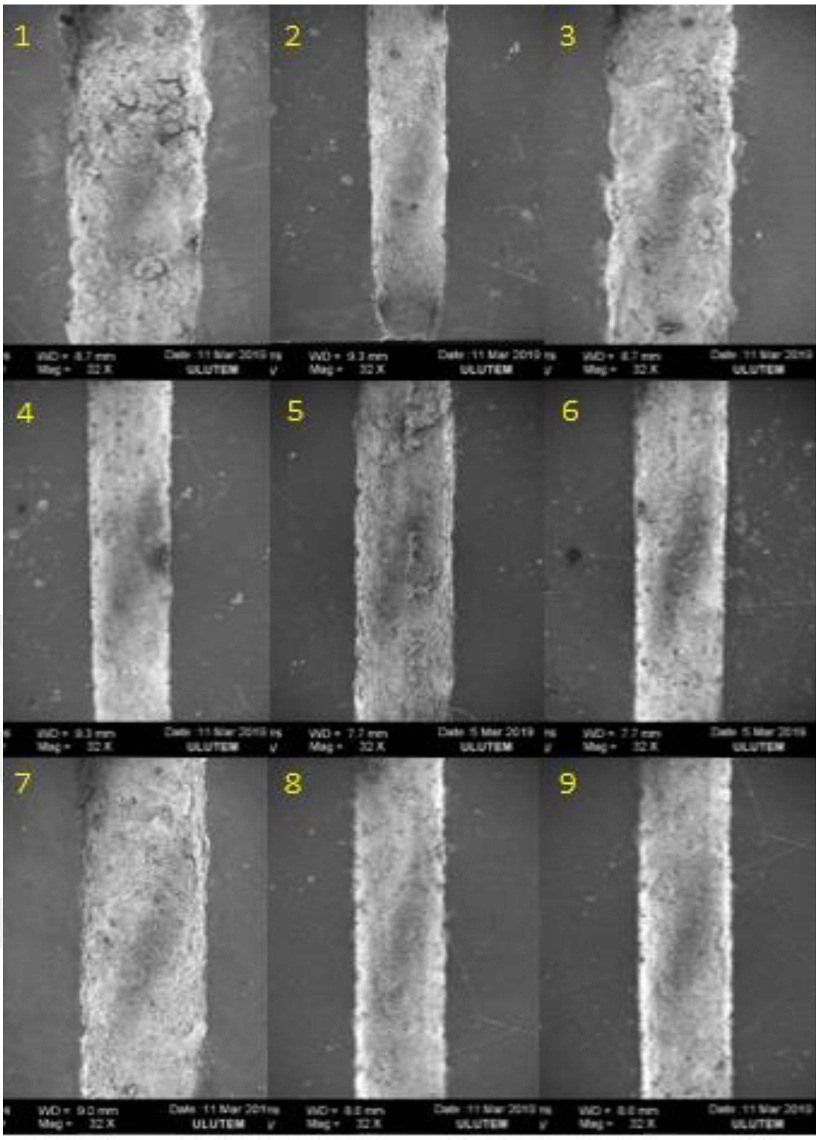

Figure 5.5 Inconel 718 Ø400μm Hole drilling experiment's SEM images

Table 5.6 Measurements of MRR, EWR, R_a / Inconel 718 / Ø300μm

Inconel 718 Ø300μm						
experimen t no:	Machine Parameters			MRR (mg/min)	EWR (mg/min)	R_a (μm)
	I (A)	T_{on} (μs)	T_{off} (μs)			
1	3,4	35	20	3,1239	1,3633	2,66
2	3,4	38	23	2,9894	2,4632	3,52
3	3,4	44	26	2,6570	2,2440	2,68
4	8,2	35	23	6,7510	3,7340	6,23
5	8,2	38	26	6,6200	3,9200	6,56
6	8,2	44	20	6,9645	3,9512	7,87
7	8,8	35	26	5,1112	5,9357	6,84
8	8,8	38	20	6,7178	6,1077	5,56
9	8,8	44	23	8,7812	6,1450	5,14

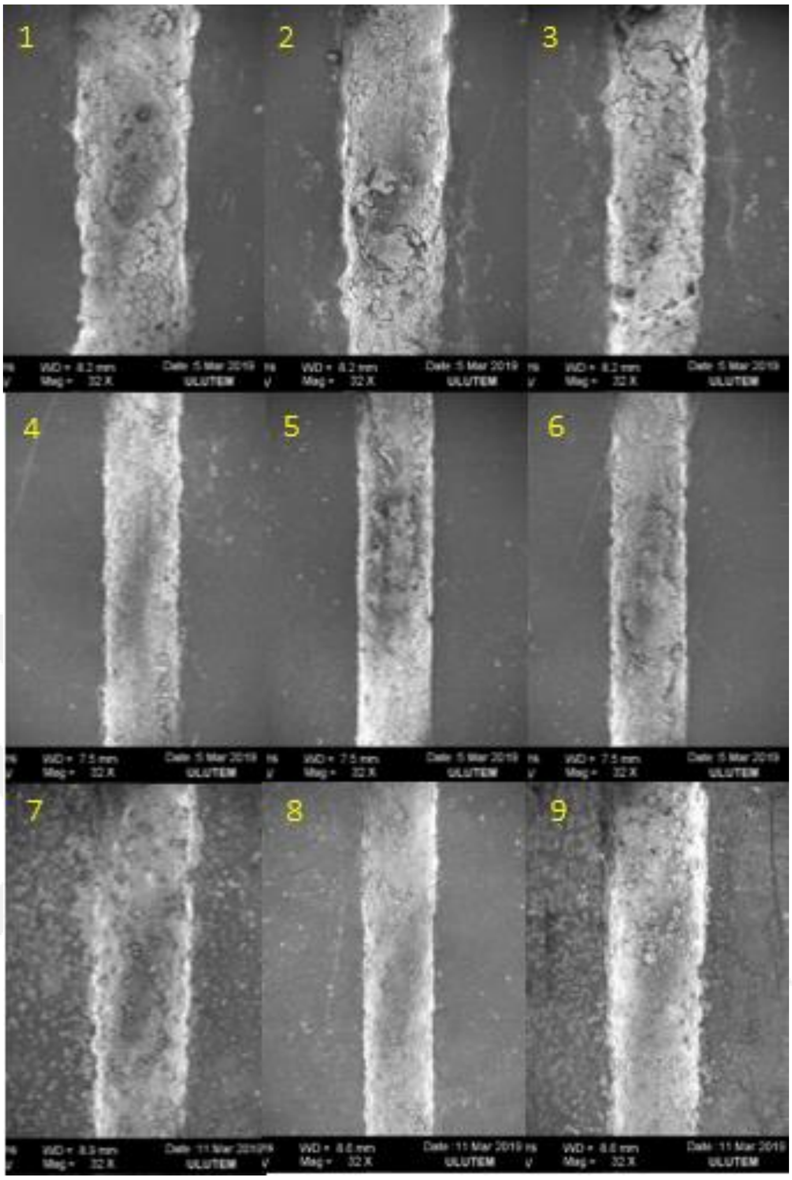

Figure 5.6 Inconel 718 Ø300µm Hole drilling experiment's SEM images

The analysis of the results which are obtained from the relevant experimental research were discussed in this section; material removal rate (MRR), electrode wear rate (EWR) and surface roughness (R_a). Results of experiments and the effects of EDM processing parameters on EDM performances were shown in Table 5.1 to Table 5.6 with numerical and shown in Figure 5.1 to 5.6 with images.

5.1.1 Machining Parameters Effects on R_a for Ti-6Al-4V

Surface roughness can be defined as surface defects which are occurs during machining. These defects are results of the inability of the sparks which were occurred. With these sparks, the material is melting and removed by coolant fluid. Molten material creates some voids on the surface where they break. These geometric defects are the undesirable characteristic consequences of EDM. Figure 5.7, Figure 5.8, Figure 5.9 presents the surface roughness measurement results. According to Figure 5.7, the roughness decreased with increasing current for all diameters. When current was selected as 3,4A the result was observed as the worst roughness value and when 8,8A was selected the best result was obtained except Ø300µm electrode results. If only Ø500µm experiments analyzed, the effect of current on surface roughness is significant. Pulse on/off time, as shown in Figure 5.8 and Figure 5.9, has no effect on surface roughness independent of diameters. When the pulse off time effect were observed (Figure 5.9), the overall image was irregular and there is no logical relationship between the parameters and response values.

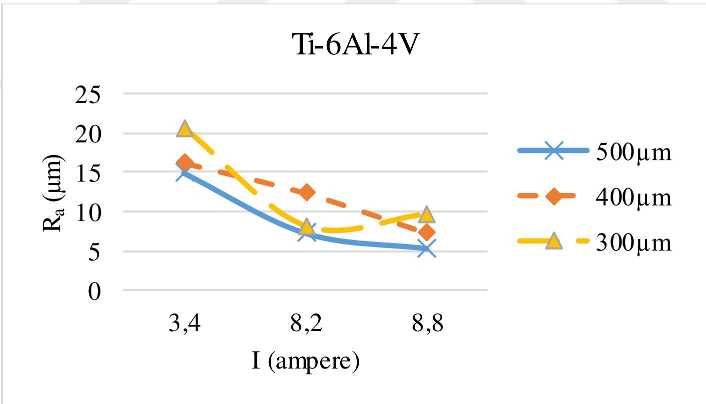

Figure 5.7 Relation between R_a and I on Ti-6Al-4V

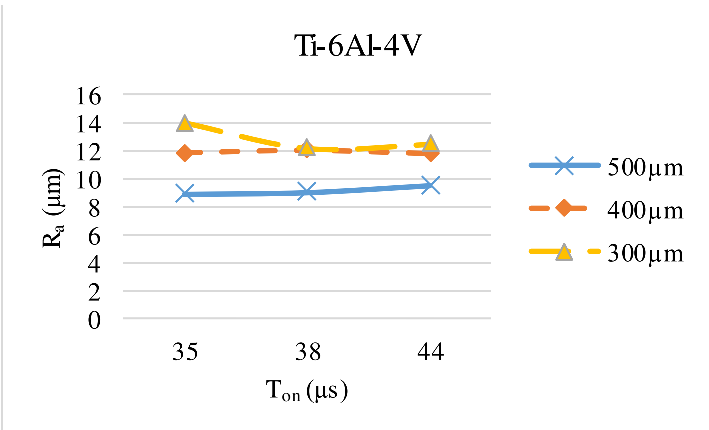

Figure 5.8 Relation between R_a and T_{on} on Ti-6Al-4V

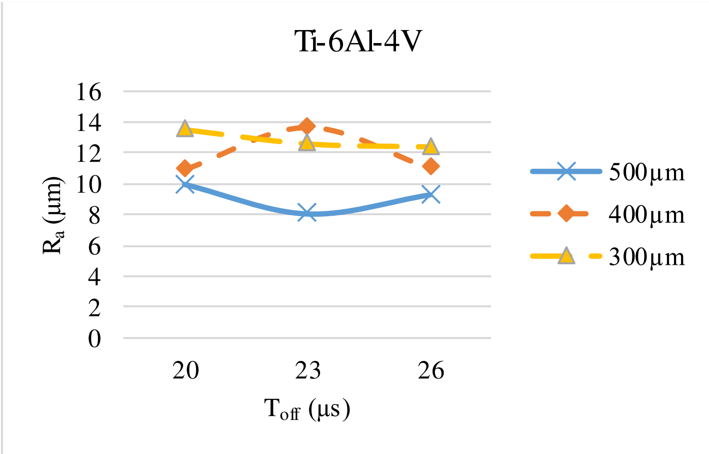

Figure 5.9 Relation between R_a and T_{off} on Ti-6Al-4V

5.1.2 Machining Parameters Effects on MRR for Ti-6Al-4V

EDM works with the principle of melting material and removing the molten material from workpiece. MRR was observed by measuring the amount of removed material. In general, MRR results in parallel with the discharge current. When current is increased, the spark energy is also increased. This increment causes the same rate of melting and evaporation on the workpiece. When Figure 5.10 was examined, a slight increase was observed from 3,4A to 8,2A at Ø300µm for MRR. A significant increase was observed between 3,4A and 8,2A at Ø500µm and a linear increase was observed at Ø400µm for all current values. According to the test results for Ø400µm, the current affected on MRR significantly. The effect of pulse on time (T_{on}) on MRR was shown in Figure 5.11. MRR was decreased when T_{on} was increased between 38µs and 44µs for Ø400µm. The increment of T_{off}, didn't cause a significant increase for Ø300µm and remained constant. However, same things cannot be said for Ø500µm. T_{on} effected on MRR regardless of diameter. When the Toff effects were observed by looking at Figure 5.12, the T_{off} increased, while MRR decreased slightly from 23µs to 26µs. There were small increases were observed between 20µs and 23µs at Ø400µm experiements. As a result, it cannot be say that T_{off} was affected on MRR significantly.

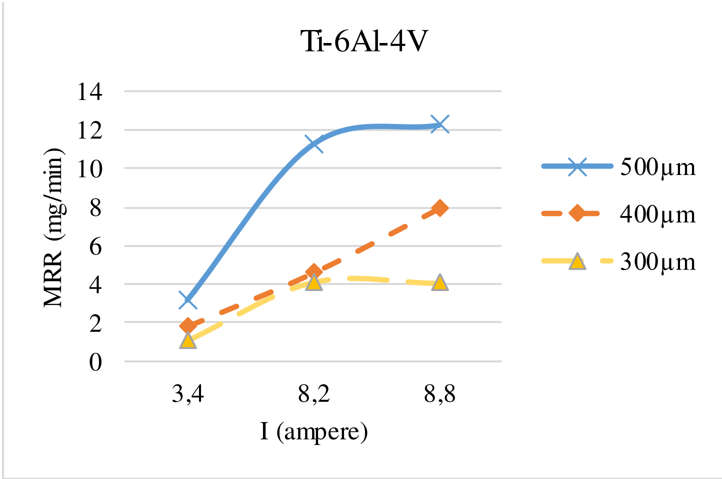

Figure 5.10 Relation between MRR and I on Ti-6Al-4V

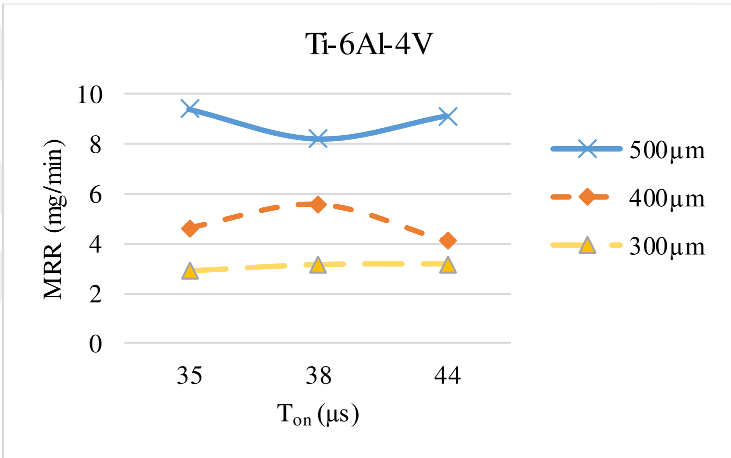

Figure 5.11 Relation between MRR and T_{on} on Ti-6Al-4V

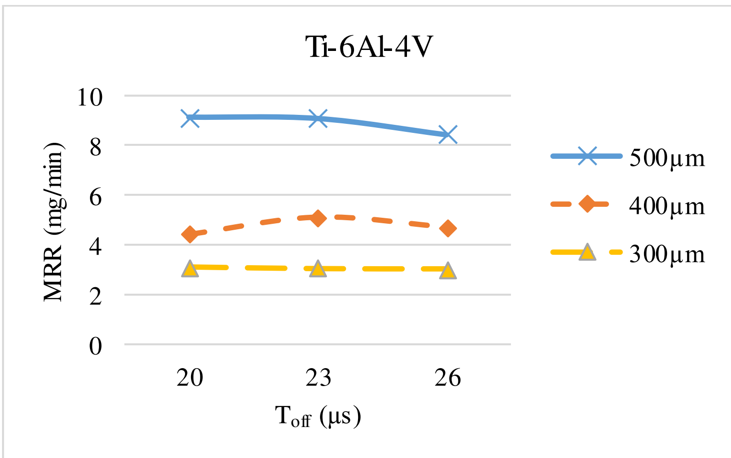

Figure 5.12 Relation between MRR and T_{off} on Ti-6Al-4V

5.1.3 Machining Parameters Effects on EWR for Ti-6Al-4V

During the EDM operation, spark occurs and corrodes the workpiece. Result of that, micro particles ejects from surface. That cause defects on the surface. In addition that, electrode melts due to the high volume of energy and consume electrode. Electrode loss is associated with EDM and electrical parameters of electrode materials and machine [17]. In this article, the effect of current, pulse on time and pulse off time on electrode wear were investigated by keep constant the capacitance (C) and voltage (V). A significant effect of current (I) on EWR was observed for experiments carried out for all diameters. When Figure 5.13 was observed for Ø500µm, EWR increased significantly at the 3,4A-8,2A range and increase slightly. The other side, Ø400um increased with a slope with constant angle while current was increased. For Ø300µm, it was observed that EWR also increased with rising current, but after reaching the maximum current value, the EWR decreased again. When T_{on} effect was examined on EWR as shown in Figure 5.14, it was observed that T_{on} at 38µs for each diameter was the same value. While T_{on} was increased, EWR slightly decreased except Ø500µm. T_{off} has slightly affected on the EWR for each diameter value as shown in Figure 5.15. Drilling with Ø500µm electrode, changing the T_{off} had small effect on the EWR. When the slope of Ø300µm was examined, it is increased firstly and decreased then. That means the EWR and T_{off} were not proportional at Ø300µm. Unlike the others, a slight increase was observed by increasing T_{off} at Ø400µm. Although Ø400µm is a larger diameter, overall electrode consumption is less than Ø300µm.

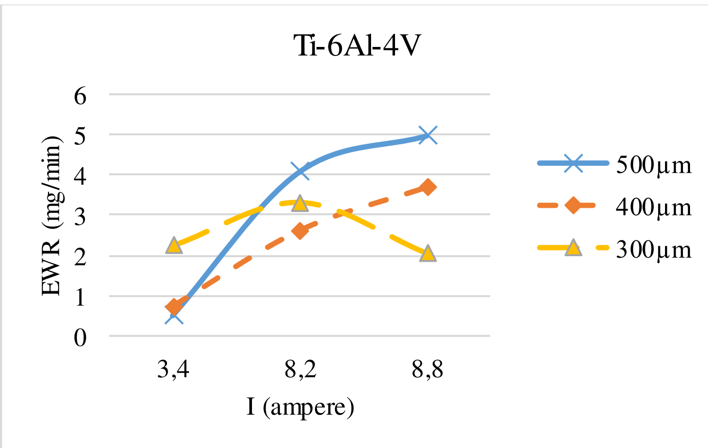

Figure 5.13 Relation between EWR and I on Ti-6Al-4V

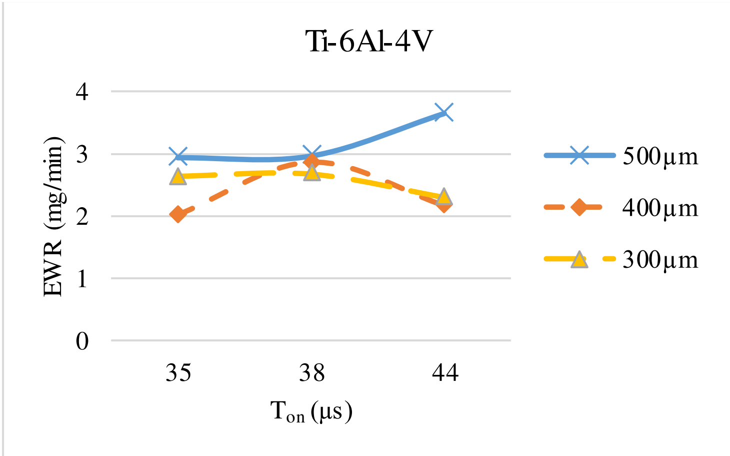

Figure 5.14 Relation between EWR and T_{on} on Ti-6Al-4V

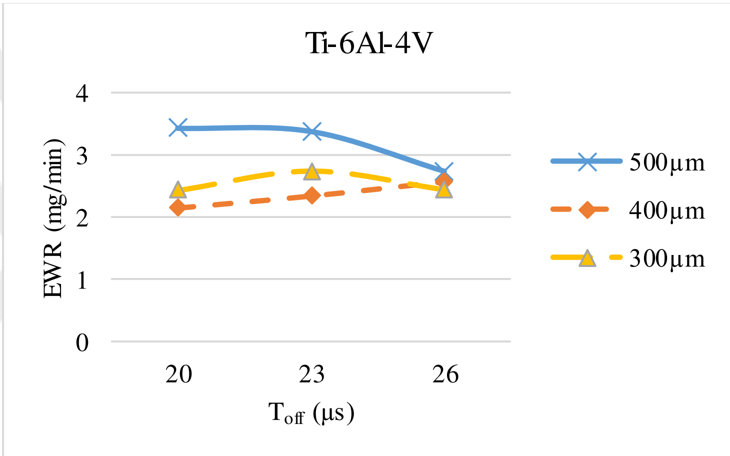

Figure 5.15 Relation between EWR and T_{off} on Ti-6Al-4V

5.1.4 Machining Parameters Effects on R_a for Inconel 718

Surface roughness can be defined as surface defects that occurs during machining. These defects are results of the inability of the sparks. With these sparks, the material is melting and removes by coolant fluid. Molten material creates some voids on the surface where they break. These geometric defects are the undesirable characteristic consequences of EDM. Figure 5.16, Figure 5.17, Figure 5.18 presents the surface roughness measurement results. According to Figure 5.16, the roughness decreased by increasing current values, like previous experiment results of Titanium alloy. When the current parameter was selected as 3,4A, observed result gives the worst roughness value, except the experiment which was made with Ø300µm. When 8,8A was selected the best result was obtained except Ø300µm again. When the result of Ø300µm experiments were observed, the best roughness values were inspected at the 3,4A among all current values. If experiments of Ø500µm were analyzed, we can say that the effect of current on surface roughness was not effective like the others. Pulse on/off time, as shown in Figure 5.17 and Figure 5.18, had no effect on surface roughness independent of diameters. When pulse off time (Figure 5.18) was observed, the overall image was regular and kept horizontal. That means there is no effect of T_{on} on R_a.

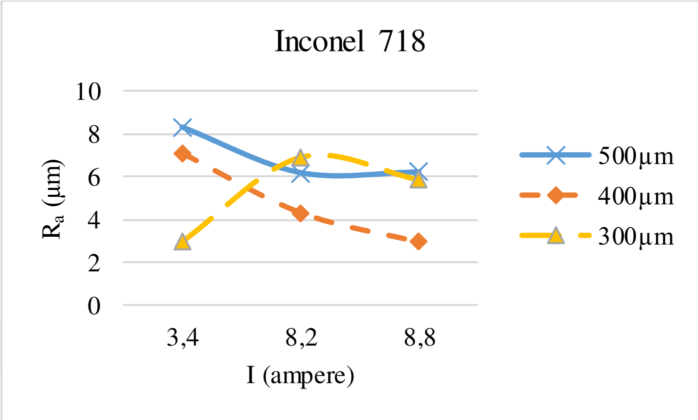

Figure 5.16 Relation between R_a and I on Inconel 718

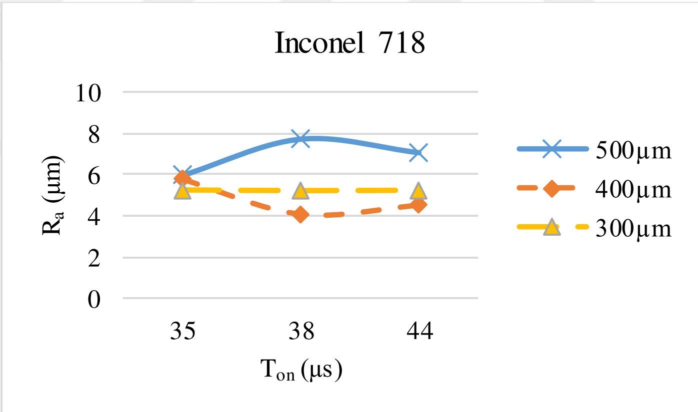

Figure 5.17 Relation between R_a and T_{on} on Inconel 718

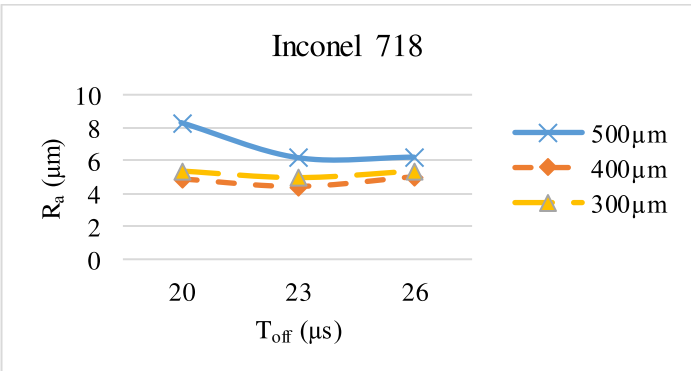

Figure 5.18 Relation between R_a and T_{off} on Inconel 718

5.1.5 Machining Parameters Effects on MRR for Inconel 718

The EDM works with the principle of melting material and removing the molten material from workpiece. The amount of molten material gives MRR. In general, MRR works parallel with the discharge current. When the current increases, spark energy increases. This increment causes proportionally melting and evaporation on workpiece. When Figure 5.19 was examined for Ø300µm, MRR increased slightly from 3,4A to 8,2A. A significant increase was observed between 3,4A and 8,2A for Ø500µm. After that, MRR decreased between 8,2A to 8,8A. According to the results of current for all diameters, current significantly affected on MRR. The effect of pulse on time (T_{on}) on MRR was shown in Figure 5.20. MRR decreased when T_{on} was increased from 38µs to 44µs for Ø500µm and Ø400µm, only increased for Ø300µm. The increment of T_{off}, not caused an increment on the drilling time for Ø400µm and Ø300µm as shown in Figure 5.21. On Ø500µm, according to experiment results, the increment was observed from 15 mg/min to 20 mg/min approximately.

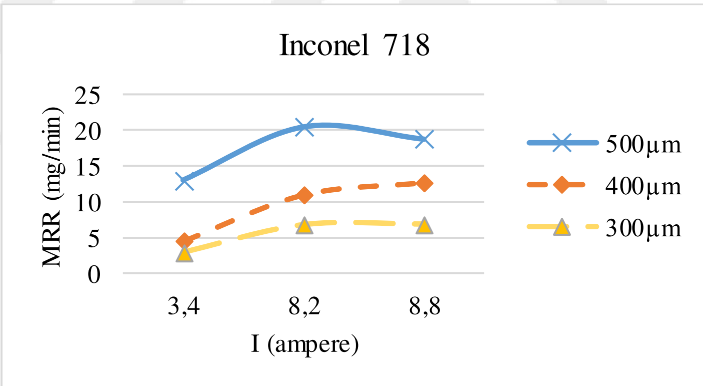

Figure 5.19 Relation between MRR and I on Inconel 718

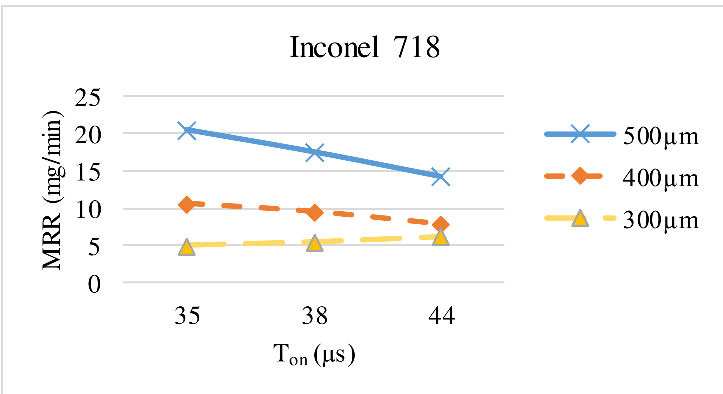

Figure 5.20 Relation between MRR and T_{on} on Inconel 718

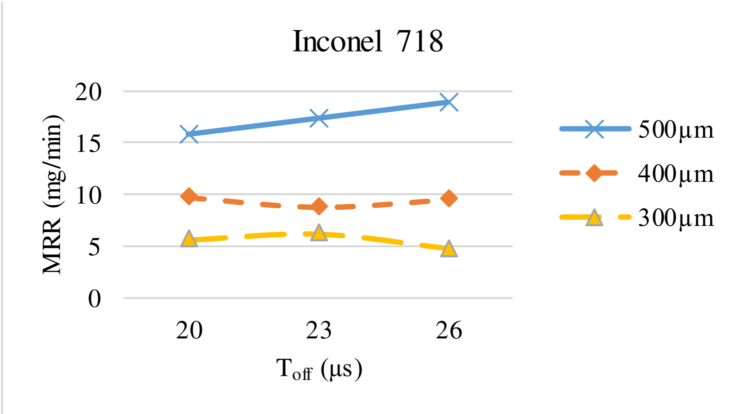

Figure 5.21 Relation between MRR and T_{off} on Inconel 718

5.1.6 Machining Parameters Effects on EWR for Inconel 718

During the EDM operation, sparks occurs and these sparks corrodes the workpiece. Result of that, micro particles ejects from surface. That cause defects on the surface. In addition that, electrode melts due to the high volume of energy and consume electrode. Electrode loss is associated with EDM and electrical parameters of electrode materials and machine [17]. In this study, the effects of current, pulse on time and pulse off time parameters on electrode wear was revealed by keeping capacitance (C) and voltage (V) constant. A significant effect of current(I) on EWR was observed for all diameter experiments (Figure 5.22). For Ø500µm, the EWR increased between 3,4A-8,2A range and continued with tiny decrease. The other side, on Ø400um experiments, EWR increased with a constant slope while the current was increased. Small decrease occured, except the last part between 8,2A to 8,8A. For Ø300µm, it was observed that EWR increased with rising current and continued with constant angle. When T_{on} effect was examined on EWR as shown in Figure 5.23, decrease of EWR observed for Ø500µm from 6 mg/min to 4 mg/min, while T_{on} increasing. For Ø400µm and Ø300µm, EWR not affected from T_{on} considerably. T_{off} has slightly affected on the EWR for Ø300µm experiments, as shown in Figure 5.24. The other experiments not effected from T_{off} considerably. When Ø400µm was examined, decreament of EWR observed and then increased again. That means the EWR and T_{off} were not proportional to Ø400µm.

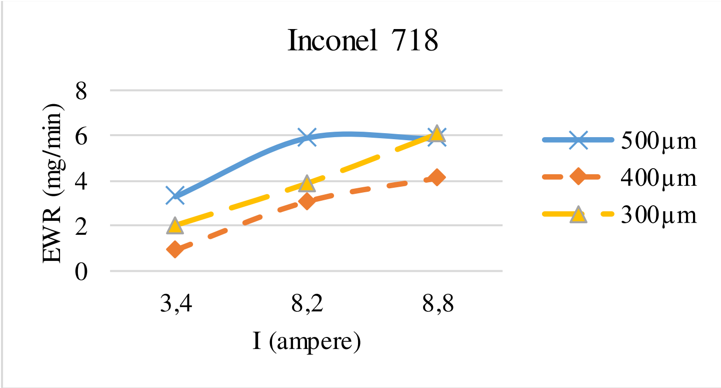

Figure 5.22 Relation between EWR and I on Inconel 718

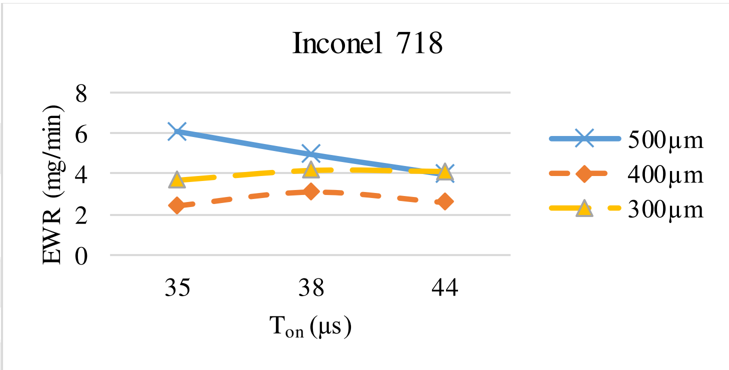

Figure 5.23 Relation between EWR and T_{on} on Inconel 718

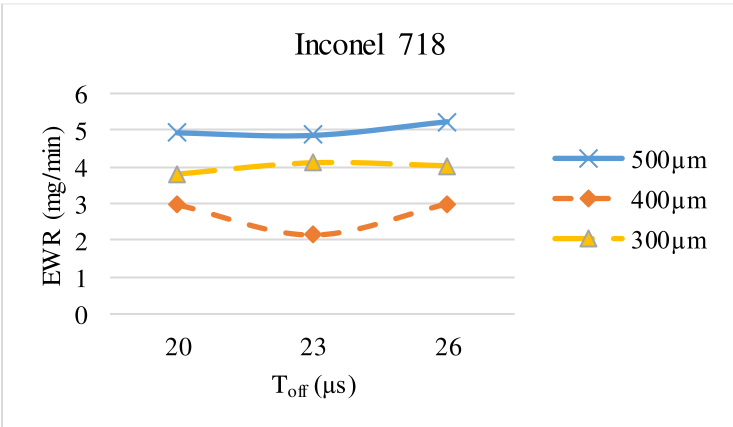

Figure 5.24 Relation between EWR and T_{off} on Inconel 718

5.2 Mathematical Modeling and Optimization of Experiment Results

5.2.1 Regression Analysis of the Experiments

Regression analysis was used to create a model for estimating the untested experimental results. The model fit is usually linear, and sometimes non-linear, such as log linear models. In this study, multiple regression analysis was used to better understand the effects of the studied parameters on response parameters. Linear regression equation was used to estimate the response parameters. For this purpose, MINITAB software was used and the process was followed. Firstly, a linear model was developed on MINITAB then analyze the parameters. The placement of the characters were done as follows.

$$\text{Response Parameter} = b0 + b1A + b2B + b3C + (\varepsilon) \quad (5.1)$$

Where b1, b2 and b3 were estimated process parameters and ε is the error. The functional correlation between response parameters and process parameters were shown by creating an empirical equation.

5.2.1.1 Regression Analysis of Ti-6Al-4V Experiments

Regression analyses were implemented for all experiments respectively and implemented for all response parameters separately. According to that, mathematical models were created using MATLAB and demonstrated the formulas which were obtained. Mathematical models should be tested to show the reliability. For each electrode dimension and belonging to that dimension's results were analyzed with ANOVA. The mathematical model and experiment results were illustrated with the graph at the same time to show the difference and closeness between them from Figure 5.25 to Figure 5.33 for Titanium alloy's experiments.

For Ti-6Al-4V -Ø500µm mathematical models;

$$MRR = 0{,}31 + 1{,}679\ I - 0{,}0033\ T_{on} - 0{,}118\ T_{off} + (\varepsilon) \quad (5.2)$$

R-sq 96,43% (Table A.1 in Appendix A)

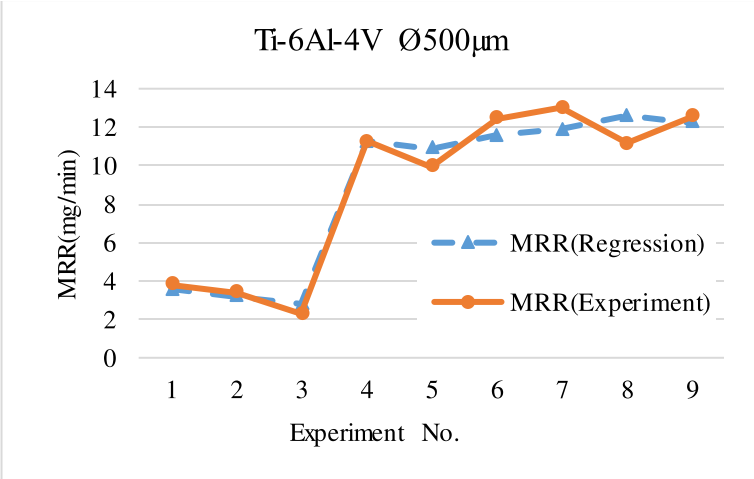

Figure 5.25 Comparison of mathematical model and experiment results of MRR for Ti-6Al-4V, Ø500µm

$$EWR = -2,85 + 0,7951\ I + 0,0839\ Ton - 0,1151\ Toff + (\varepsilon) \quad (5.3)$$

R-sq 98,27% (Table A.2 in Appendix A)

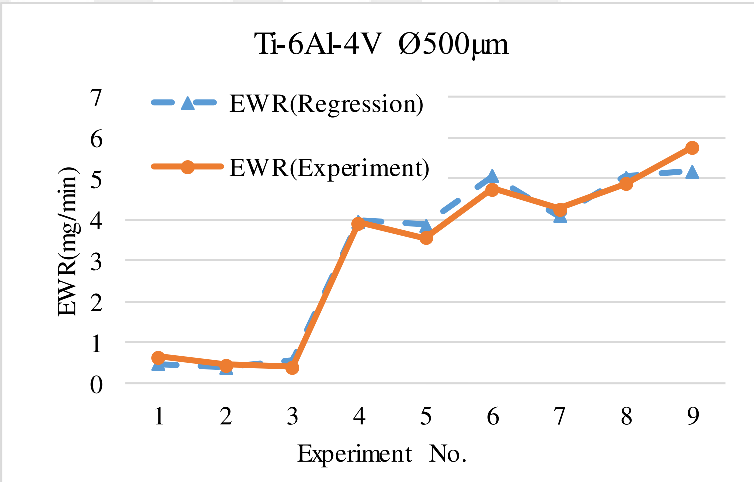

Figure 5.26 Comparison of mathematical model and experiment results of EWR for Ti-6Al-4V, Ø500µm

$$Ra = 20,56 - 1,707\ I + 0,071\ Ton - 0,113\ Toff + (\varepsilon) \quad (5.4)$$

R-sq 92,01% (Table A.3 in Appendix A)

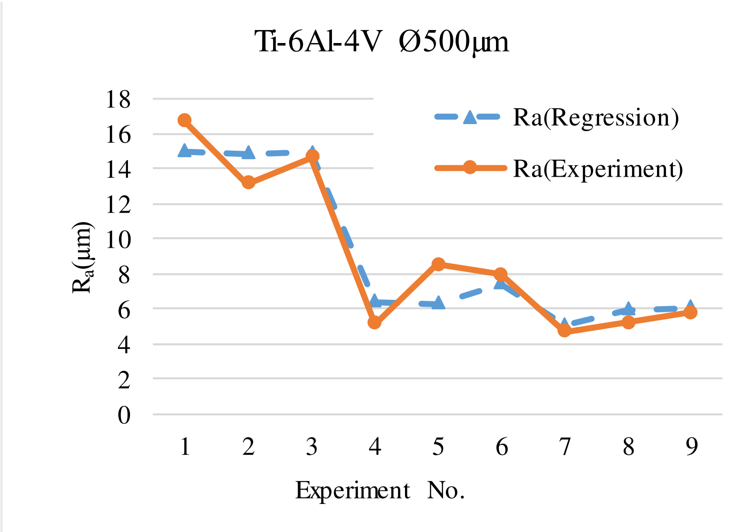

Figure 5.27 Comparison of mathematical model and experiment results of R_a for Ti-6Al-4V, Ø500µm

For Ti-6Al-4V -Ø400µm mathematical models;

$$MRR\ (mg/min) = 0{,}71 + 0{,}918\ I - 0{,}086\ Ton + 0{,}049\ Toff + (\varepsilon) \quad (5.5)$$

R-sq 98,17% (Table A.4 in Appendix A)

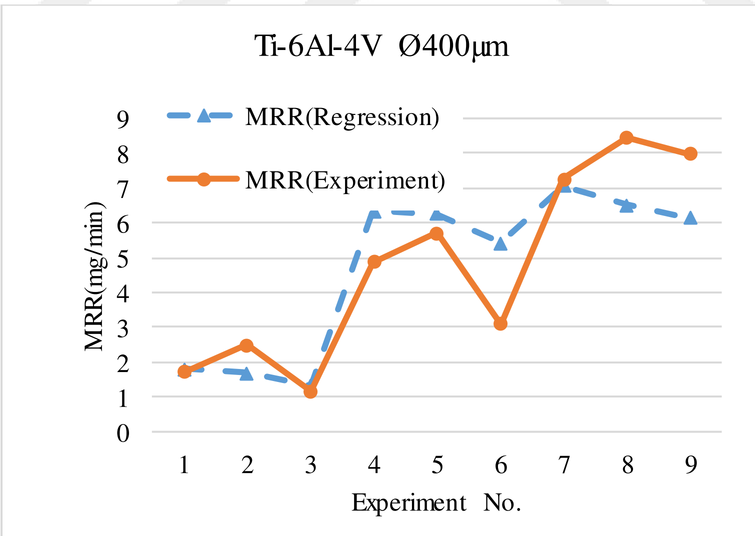

Figure 5.28 Comparison of mathematical model and experiment results of MRR for Ti-6Al-4V, Ø400µm

$$EWR\ (mg/min) = -2{,}50 + 0{,}4878\ I - 0{,}0024\ T_{on} + 0{,}0705\ T_{off} + (\varepsilon) \quad (5.6)$$

R-sq 98,64% (Table A.5 in Appendix A)

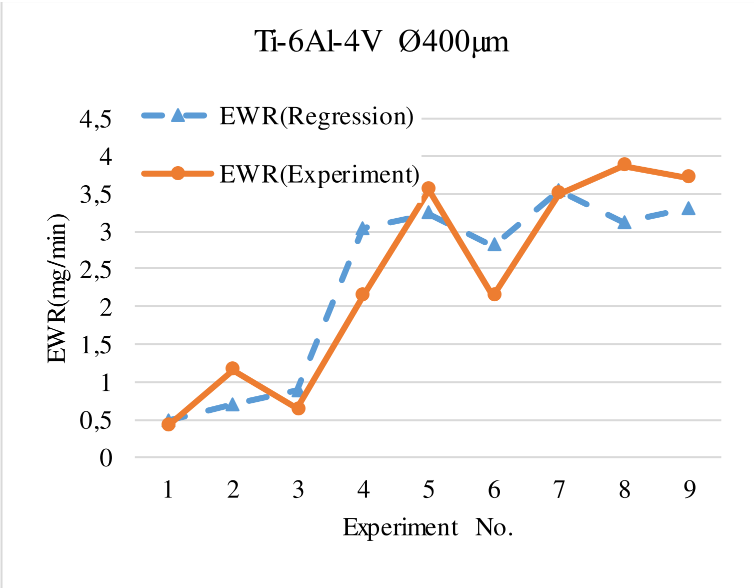

Figure 5.29 Comparison of mathematical model and experiment results of EWR for Ti-6Al-4V, Ø400µm

$$R_a\ (\mu m) = 20{,}9 - 1{,}324\ I - 0{,}011\ T_{on} + 0{,}017\ T_{off} + (\varepsilon) \quad (5.7)$$

R-sq 88,24% (Table A.6 in Appendix A)

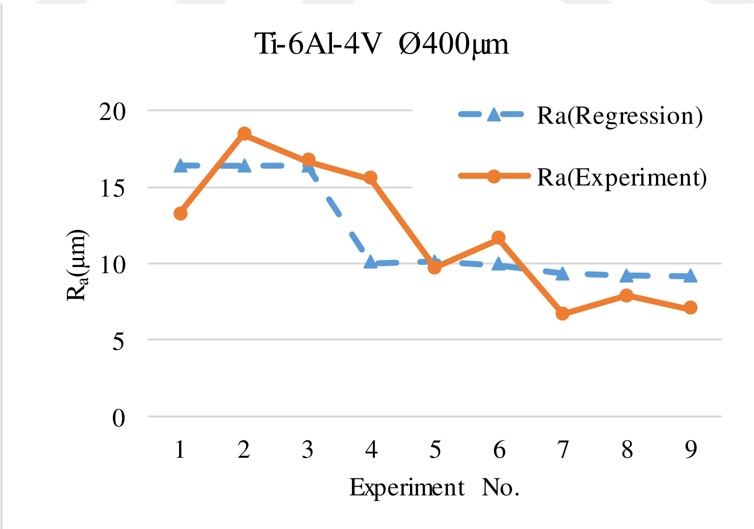

Figure 5.30 Comparison of mathematical model and experiment results of R_a for Ti-6Al-4V, Ø400µm

For Ti-6Al-4V -Ø300µm mathematical models;

$$MRR\ (mg/min) = -1{,}68 + 0{,}5819\ I + 0{,}0276\ T_{on} - 0{,}0127\ T_{off} + (\varepsilon) \quad (5.8)$$

R-sq 97,94% (Table A.7 in Appendix A)

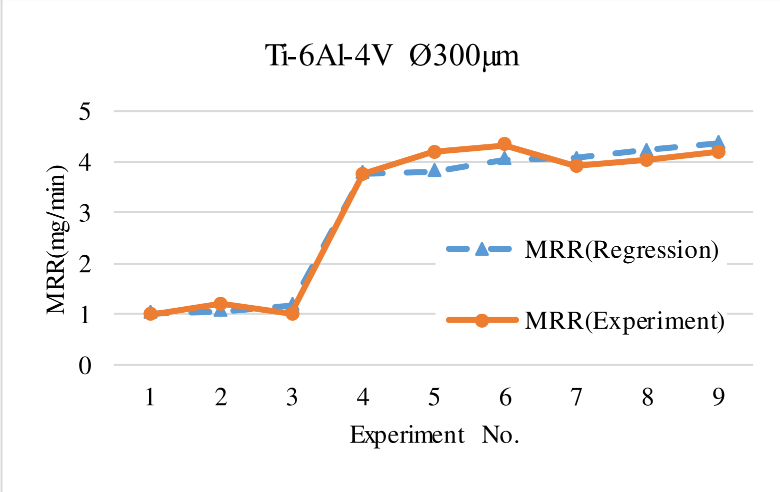

Figure 5.31 Comparison of mathematical model and experiment results of MRR for Ti-6Al-4V, Ø300µm

$$EWR\ (mg/min) = 3{,}65 + 0{,}065\ I - 0{,}0412\ T_{on} + 0{,}002\ T_{off} + (\varepsilon) \qquad (5.9)$$

R-sq 91,90% (Table A.8 in Appendix A)

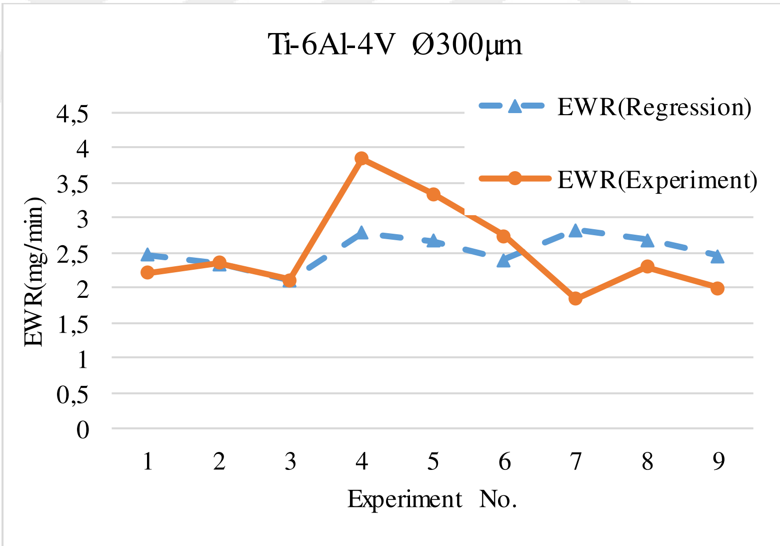

Figure 5.32 Comparison of mathematical model and experiment results of EWR for Ti-6Al-4V, Ø300µm

$$R_a\ (\mu m) = 37{,}9 - 2{,}253\ I - 0{,}140\ T_{on} - 0{,}186\ T_{off} + (\varepsilon) \qquad (5.10)$$

R-sq 91,44% (Table A.9 in Appendix A)

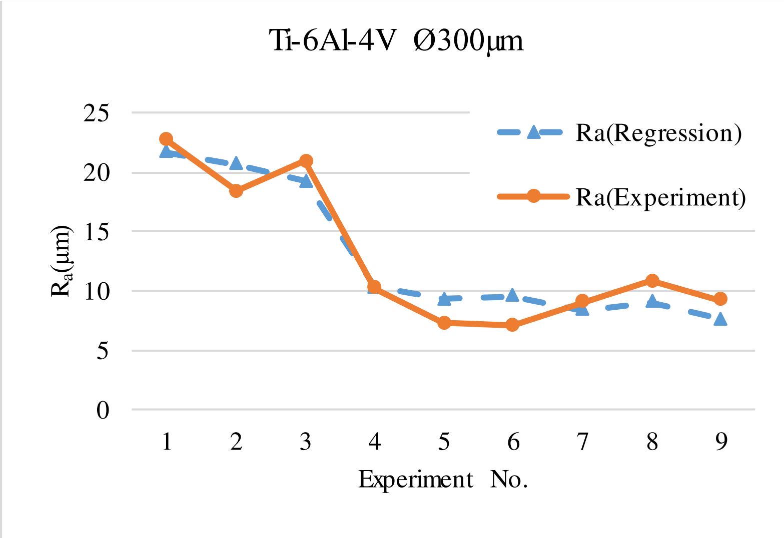

Figure 5.33 Comparison of mathematical model and experiment results of R_a for Ti-6Al-4V, Ø300µm

5.2.1.2 Regression Analysis of Inconel 718 Experiments

Regression analyses were implemented for all experiments respectively and implemented for all response parameters separately for Inconel 718 experiments also. The mathematical model and experiment results were illustrated with the graph at the same time to show the difference and closeness between them. The error could be observed easily as shown in figures from Figure 5.34 to 5.42 for Inconel 718 experiments.

For Inconel 718-Ø500µm mathematical models;

$$MRR\ (mg/min) = 23{,}41 + 1{,}247\ I - 0{,}676\ T_{on} + 0{,}516\ T_{off} + (\varepsilon) \quad (5.11)$$

R-sq 92,88% (Table B.1 in Appendix B)

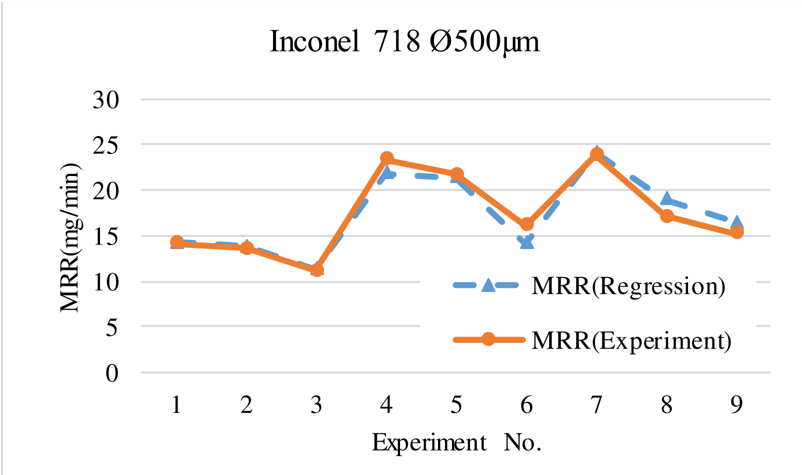

Figure 5.34 Comparison of mathematical model and experiment results of MRR for Inconel 718, Ø500µm

$$EWR\ (mg/min) = 9,24 + 0,4989\ I - 0,2253\ T_{on} + 0,0505\ T_{off} + (\varepsilon) \tag{5.12}$$

R-sq 89,95% (Table B.2 in Appendix B)

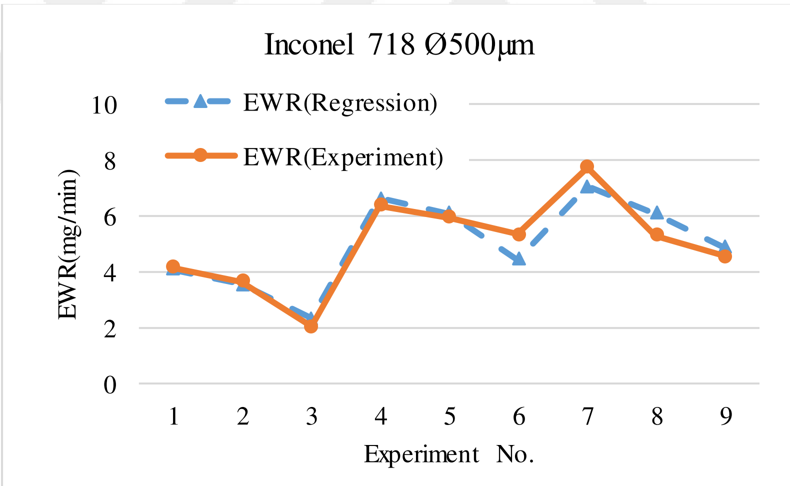

Figure 5.35 Comparison of mathematical model and experiment results of EWR for Inconel 718, Ø500µm

$$R_a\ (\mu m) = 4,30 + 1,026\ I + 0,130\ T_{on} - 0,406\ T_{off} + (\varepsilon) \tag{5.13}$$

R-sq 79,66% (Table B.3 in Appendix B)

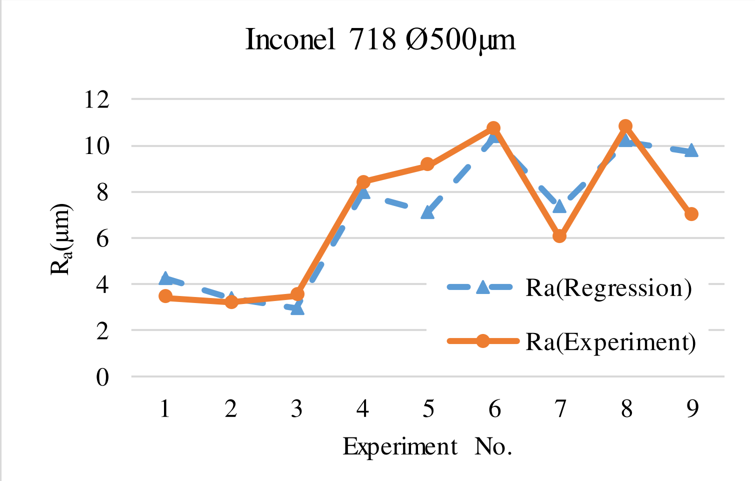

Figure 5.36 Comparison of mathematical model and experiment results of R_a for Inconel 718, Ø500µm

For Inconel 718-Ø400µm mathematical models;

$$MRR\ (mg/min) = 12{,}04 + 1{,}455\ I - 0{,}3018\ T_{on} - 0{,}036\ T_{off} + (\varepsilon) \qquad (5.14)$$

R-sq 97,20% (Table B.4 in Appendix B)

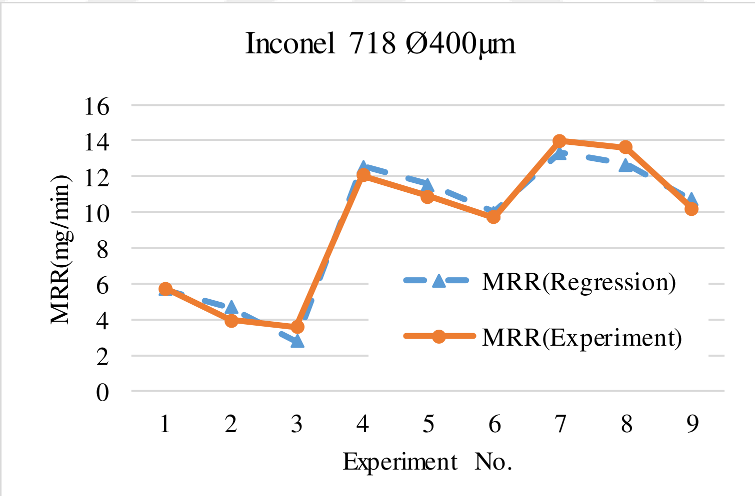

Figure 5.37 Comparison of mathematical model and experiment results of MRR for Inconel 718, Ø400µm

$$EWR\ (mg/min) = -1{,}16 + 0{,}534\ I + 0{,}0037\ T_{on} + 0{,}004\ T_{off} + (\varepsilon) \qquad (5.15)$$

R-sq 80,18% (Table B.5 in Appendix B)

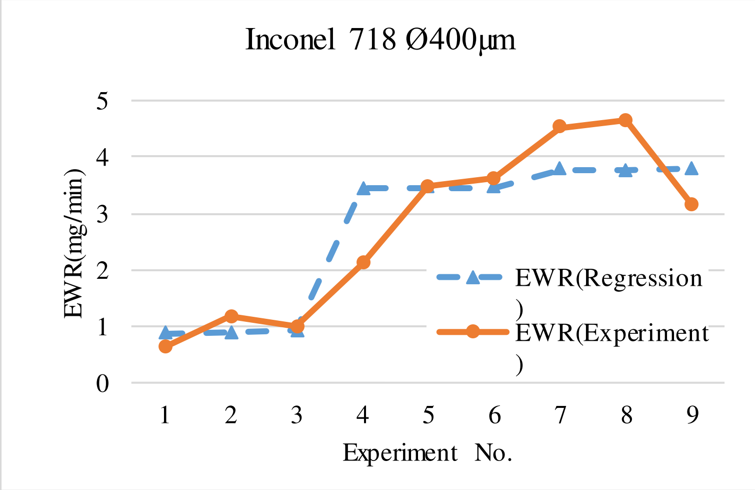

Figure 5.38 Comparison of mathematical model and experiment results of EWR for Inconel 718, Ø400µm

$$R_a\ (\mu m) = 13{,}29 - 0{,}696\ I - 0{,}110\ T_{on} + 0{,}022\ T_{off} + (\varepsilon) \quad (5.16)$$

R-sq 78,46 (Table B.6 in Appendix B)

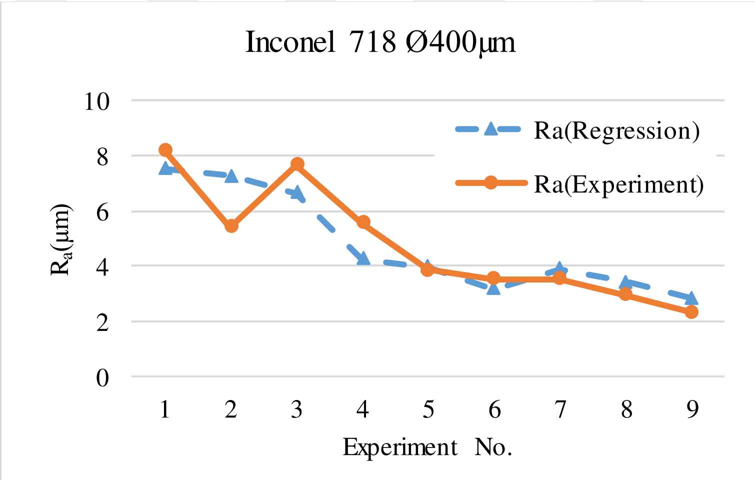

Figure 5.39 Comparison of mathematical model and experiment results of R_a for Inconel 718, Ø400µm

For Inconel 718-Ø300µm mathematical models;

$$MRR\ (mg/min) = -1{,}42 + 0{,}759\ I + 0{,}1249\ T_{on} - 0{,}134\ T_{off} + (\varepsilon) \quad (5.17)$$

R-sq 88,76% (Table B.7 in Appendix B)

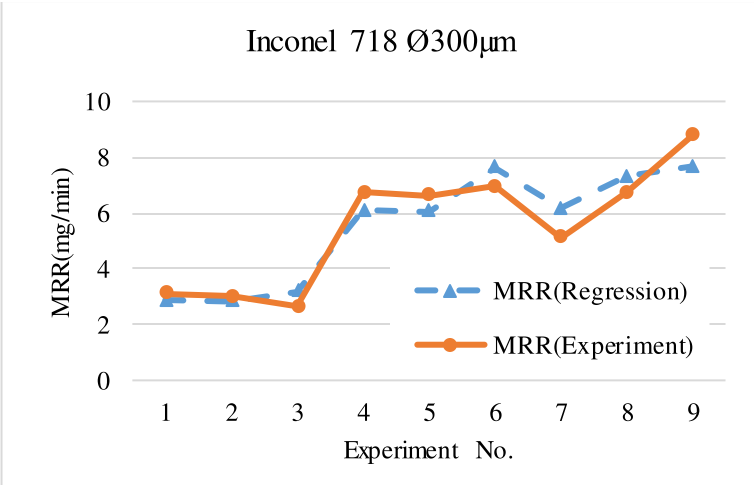

Figure 5.40 Comparison of mathematical model and experiment results of MRR for Inconel 718 Ø300µm

$$EWR\ (mg/min) = -2,59 + 0,609\ I + 0,0403\ T_{on} + 0,038\ T_{off} + (\varepsilon) \qquad (5.18)$$

R-sq 78,15% (Table B.8 in Appendix B)

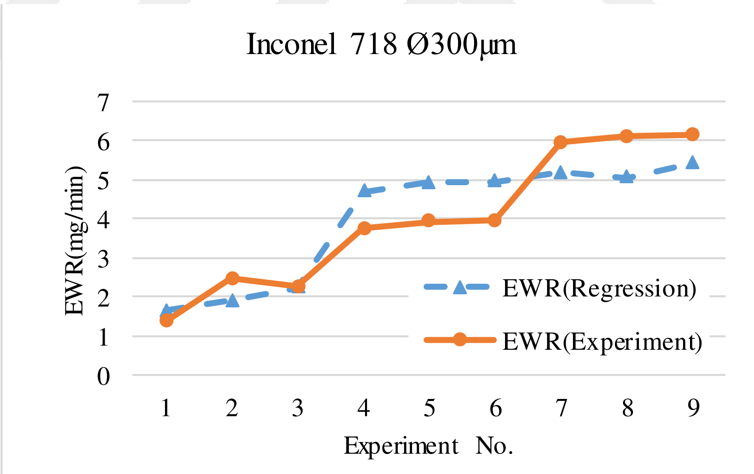

Figure 5.41 Comparison of mathematical model and experiment results of EWR for Inconel 718, Ø300µm

$$R_a\ (\mu m) = 0,89 + 0,645\ I - 0,001\ T_{on} - 0,001\ T_{off} + (\varepsilon) \qquad (5.19)$$

R-sq 76,68% (Table B.9 in Appendix B)

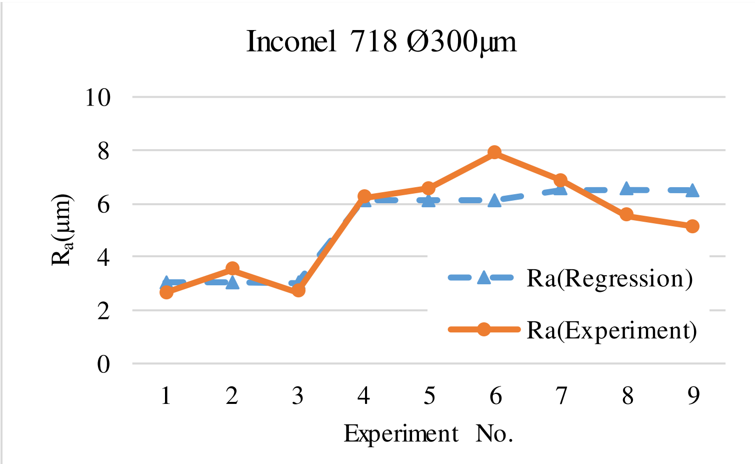

Figure 5.42 Comparison of mathematical model and experiment results of R_a for Inconel 718, Ø300µm

5.2.2 Optimization Results of Ti-6Al-4V Experiments

5.2.2.1 Optimization of Ti-6Al-4V Drilled with Ø500µm

Figure 4.43 shows the optimization plots of Ti-6Al-4V drilled with Ø500µm for MRR, EWR and R_a and optimum results. These results were summarized as below.

I =8.1297 A, T_{on} =35 µs, T_{off} =26 µs

The nearest machining settings can set as;

I ≈ 8.2 A, T_{on} =35 µs, T_{off} =26 µs

Combined or composite desirability of the three responses is D=0.6579

Predict responses which were obtained from mathematical equations;

R_a=6.08µm MRR=10.8898 mg/min EWR=3.6109 mg/min (Figure 5.44)

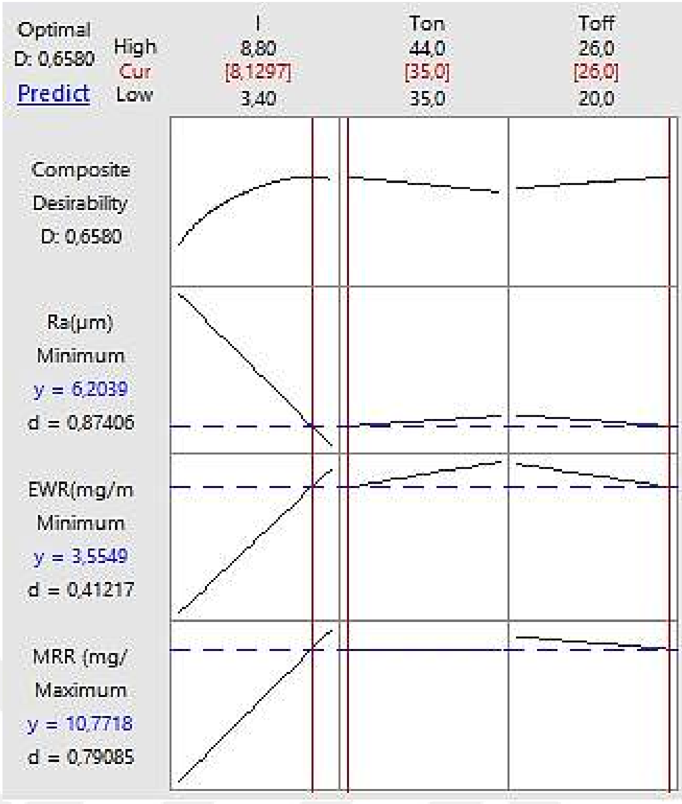

Figure 5.43 Response optimizer toolkit result for Ø500µm

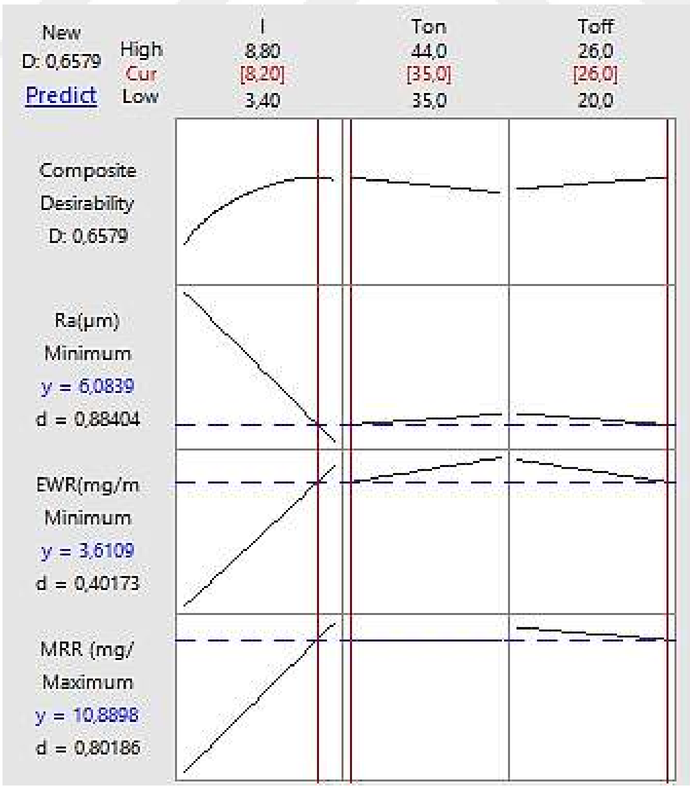

Figure 5.44 Modified results for Ø500µm

5.2.2.2 Optimization of Ti-6Al-4V Drilled with Ø400µm

Figure 5.45 shows the optimization plots of Ti-6Al-4V drilled with Ø400µm for MRR, EWR and R_a and optimum results. These results were summarized as below.

I =7.6545 A, T_{on} =35 µs, T_{off} =20 µs

The nearest machining settings could set as;

I ≈ 8.2 A, T_{on} =35 µs, T_{off} =20 µs

Combined or composite desirability of the three responses is D=0.5313

Predict responses which were obtained from mathematical equations;

R_a=10.0001µm MRR=6.2313 mg/min EWR=2.8295 mg/min (Figure 5.46)

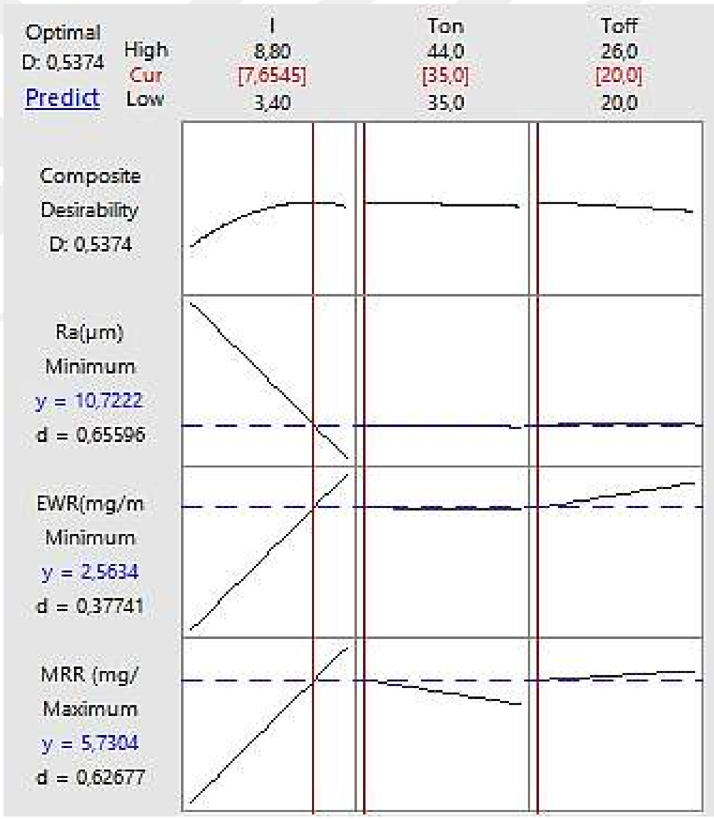

Figure 5.45 Response optimizer toolkit result for Ø400µm

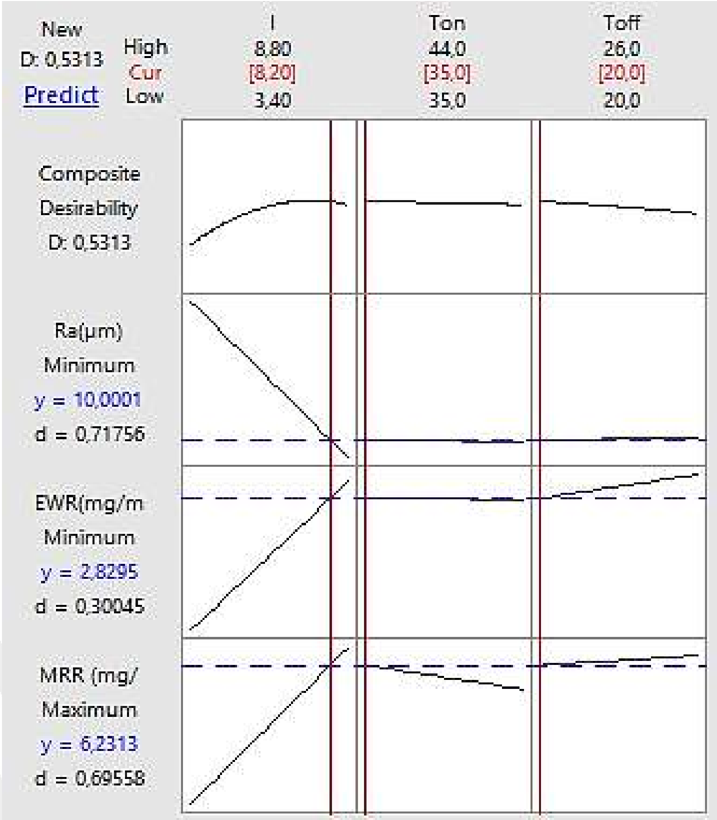

Figure 5.46 Modified results for Ø400µm

5.2.2.3 Optimization of Ti-6Al-4V Drilled with Ø300µm

Figure 5.47 shows the optimization plots of Ti-6Al-4V which were drilled with Ø300µm for MRR, EWR and R_a and optimum results. These results were summarized as below.

I =8.8 A, T_{on} =44 µs, T_{off} =26 µs

The nearest machining settings can set as;

I ≈ 8.8 A, T_{on} =44 µs, T_{off} =26 µs

Combined or composite desirability of the three responses is D=0.8834

Predict responses which were obtained from mathematical equations;

R_a=7.0657 µm MRR=4.3263 mg/min EWR=2.4644 mg/min (Figure 5.48)

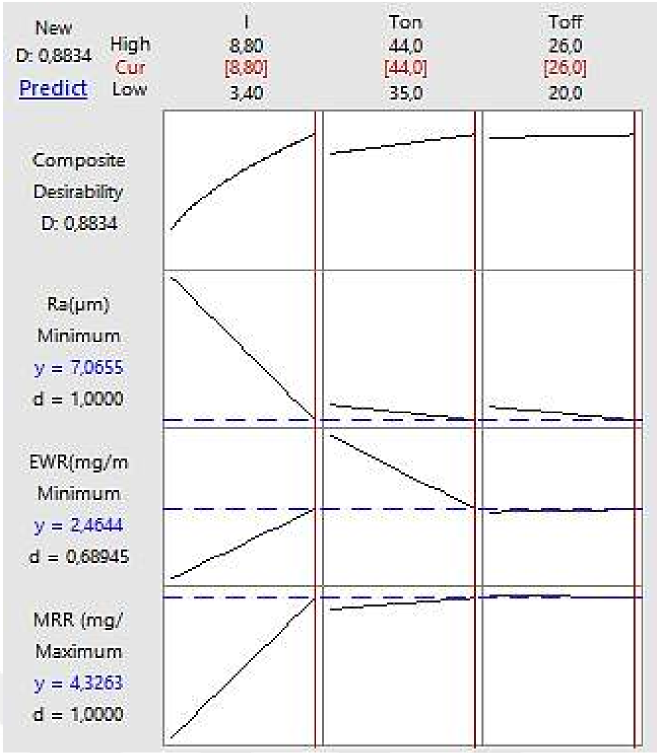

Figure 5.47 Response optimizer toolkit result for Ø300µm

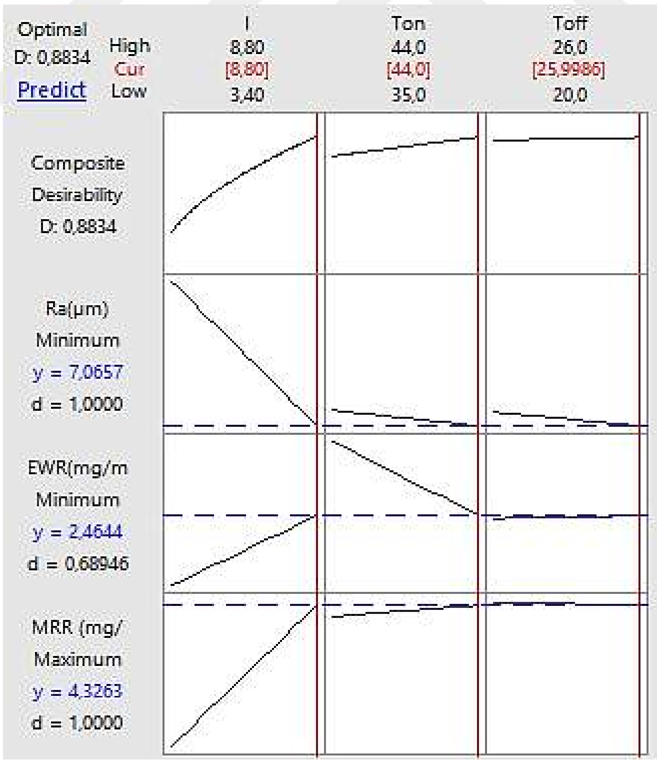

Figure 5.48 Modified results for Ø300µm

5.2.3 Optimization Results of Inconel 718 Experiments

5.2.3.1 Optimization of Inconel 718 Drilled with Ø500µm

Figure 5.49 shows the optimization plots of Inconel 718 drilled with Ø500µm for MRR, EWR and R_a and optimum results. These results were summarized as below.

I =4.2727 A, T_{on} =35 µs, T_{off} =26 µs

The nearest machining settings can set as;

I ≈ 3.40 A, T_{on} =35 µs, T_{off} =26 µs

Combined or composite desirability of the three responses is D=0.5334

Predict responses which were obtained from mathematical equations;

R_a=1.7841 µm MRR=17.4069 mg/min EWR=4.3616 mg/min (Figure 5.50)

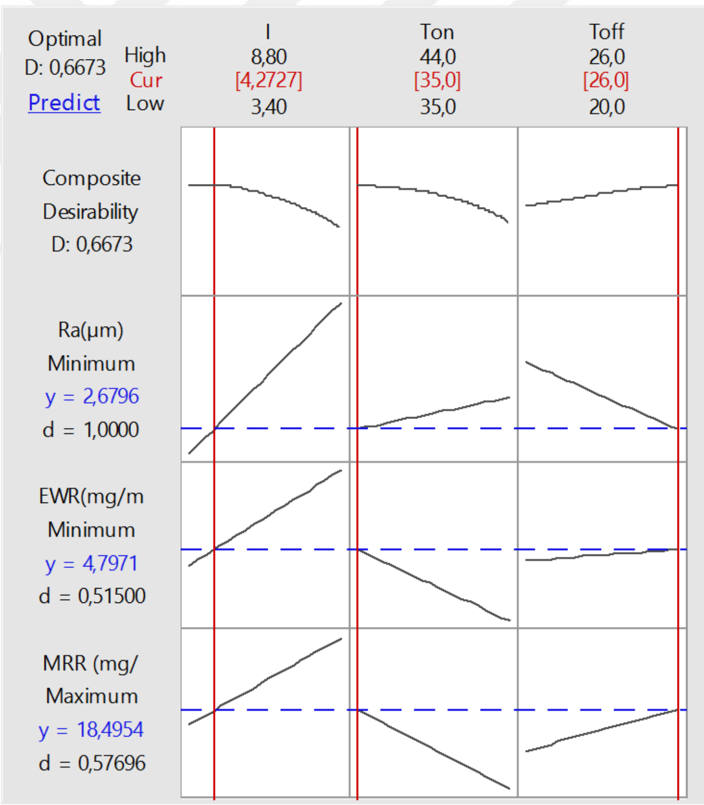

Figure 5.49 Response optimizer toolkit result for Ø500µm

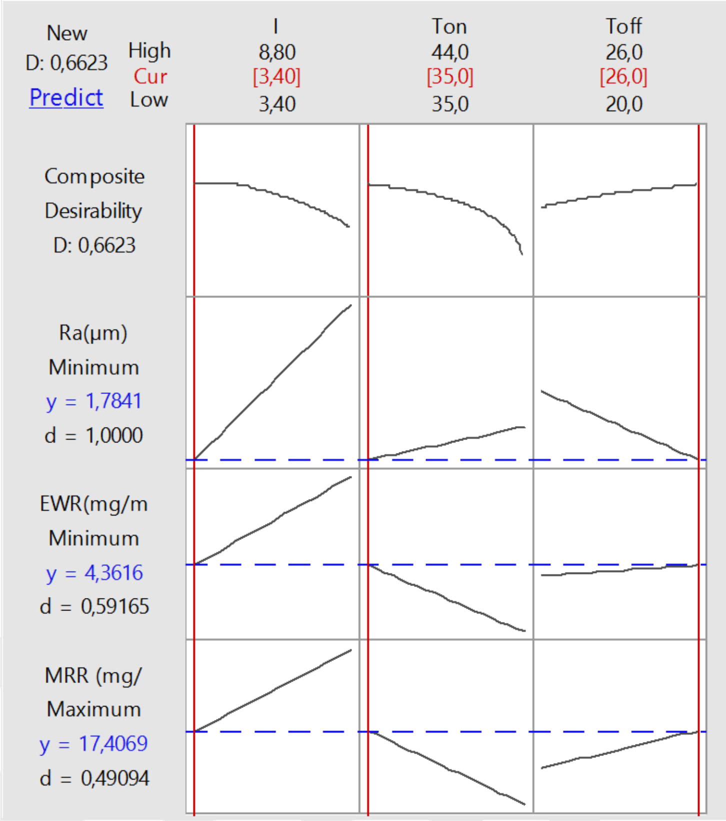

Figure 5.50 Modified results for Ø500µm

5.2.3.2 Optimization of Inconel 718 Drilled with Ø400µm

Figure 5.51 shows the optimization plots of Inconel 718 drilled with Ø400µm for MRR, EWR and R_a and optimum results. These results were summarized as below.

I =7.7347 A, T_{on} =35 µs, T_{off} =20 µs

The nearest machining settings can set as;

I ≈ 8.2 A, T_{on} =35 µs, T_{off} =20 µs

Combined or composite desirability of the three responses is D=0.5670

Predict responses which were obtained from mathematical equations;

R_a=4.1756 µm MRR=12.6762 mg/min EWR=3.4238 mg/min (Figure 5.52)

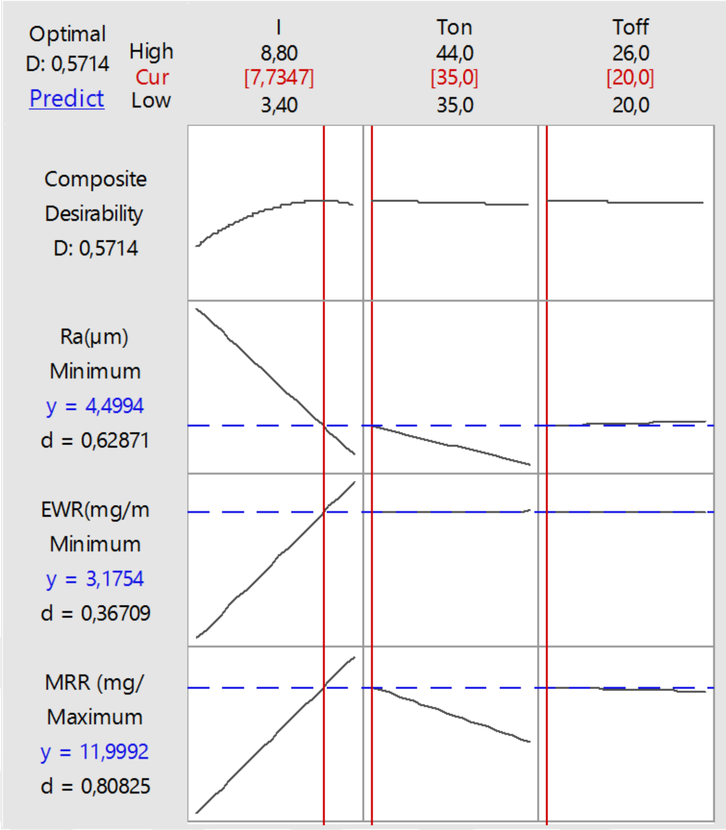

Figure 5.51 Response optimizer toolkit result for Ø400µm

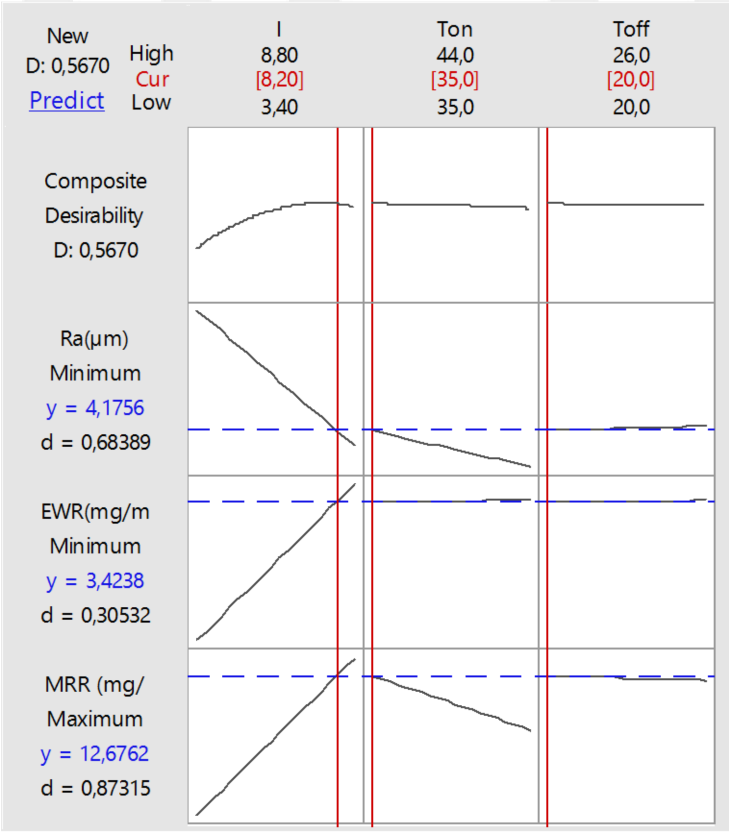

Figure 5.52 Modified results for Ø400µm

5.2.3.3 Optimization of Inconel 718 Drilled with Ø300µm

Figure 5.53 shows the optimization plots of Inconel 718 drilled with Ø300µm for MRR, EWR and R_a and optimum results. These results were summarized as below.

I =5.1340 A, T_{on} =35 µs, T_{off} =20 µs

The nearest machining settings can set as;

I ≈ 3.40 A, T_{on} =35 µs, T_{off} =20 µs

Combined or composite desirability of the three responses is D=0.5269

Predict responses which were obtained from mathematical equations;

R_a=3.0424 µm MRR=3.3790 mg/min EWR=1.6418 mg/min (Figure 5.54)

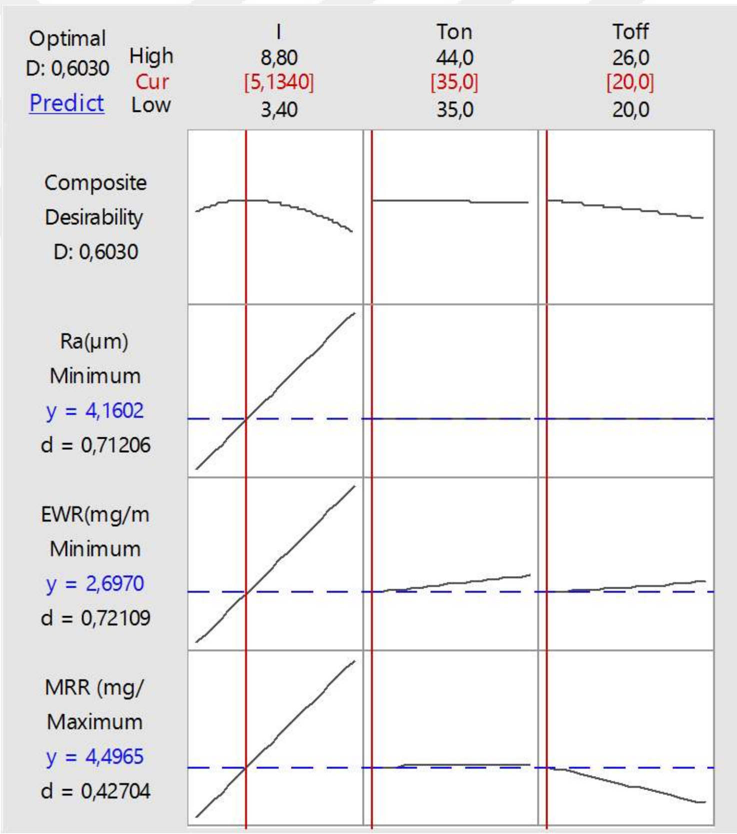

Figure 5.53 Response optimizer toolkit result for Ø300µm

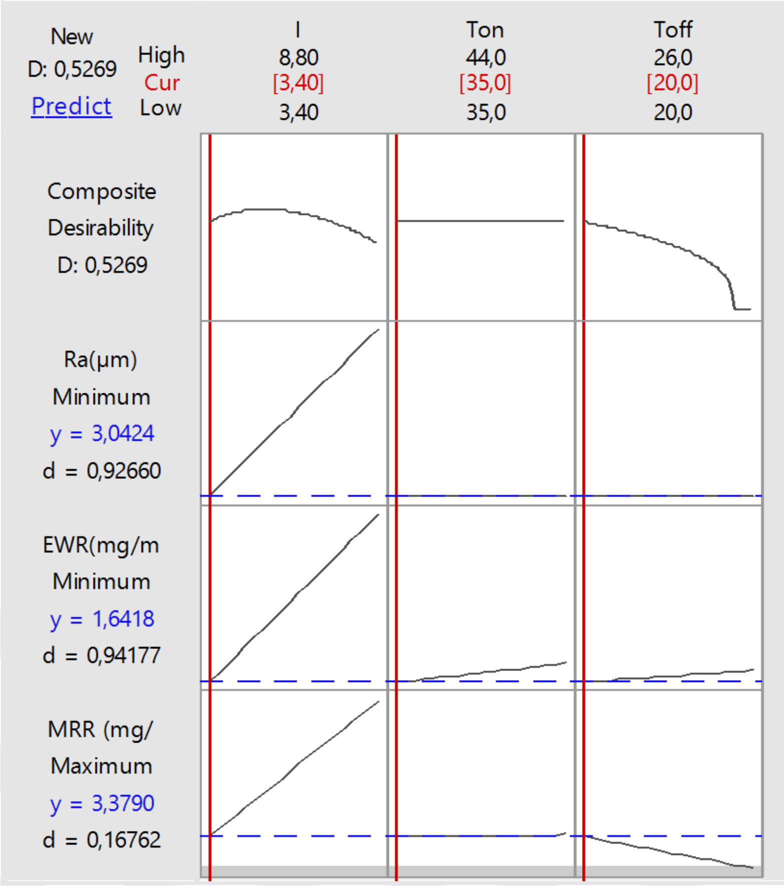

Figure 5.54 Modified results for Ø300µm

5.2.4 Validation Experiments

Validation experiments were performed to determine the reliability of the designed mathematical models and output parameters results. In this direction, 3 different experiments (these experiments were chosen according to experiment results which were desire most) were performed with double time and output parameters results were measured. Test parameters were designed and results were shown according to these parameters which were shown at Table 5.7 for Titanium alloy's experiments and at Table 5.9 for Nickel alloy's experiments. The difference between the results was expressed as a percentage at Table 5.8 for Titanium alloy's experiments and at Table 5.10 for Nickel alloy's experiments.

Table 5.7 Validation experiment's parameters of Ti-6Al-4V

Exp. No	Machining Parameters				MRR(mg/min)	EWR(mg/min)	R_a(µm)
	I(A)	T_{on}(µs)	T_{off}(µs)	D(µm)			
1	8.2	35	26	500	4,6823	1,3756	6,635
2	8.2	35	26	500	5,3667	1,3337	8,15
3	8.2	35	20	400	4,0462	1,2621	10,39
4	8.2	35	20	400	3,3112	1,3356	8,045
5	8.8	44	26	300	2,7630	0,9298	7,41
6	8.8	44	26	300	2,3391	1,3908	9,96

Table 5.8 Comparison of the validation experiments and mathematical results of Ti-6Al-4V

	Experimental			Mathematical			Error		
Exp. No	MRR (mg/min)	EWR (mg/min)	R_a(µm)	MRR (mg/min)	EWR (mg/min)	R_a(µm)	MRR(%)	EWR(%)	R_a(%)
1	4,6823	1,3756	6,6350	10,8898	3,6109	6,0800	132,57	162,50	-8,36
2	5,3668	1,3338	8,1500	10,8898	3,6109	6,0800	102,91	170,73	-25,40
3	4,0463	1,2621	10,3900	6,2313	2,8295	10,0001	54,00	124,18	-3,75
4	3,3112	1,3356	8,0450	6,2313	2,8295	10,0001	88,19	111,85	24,30
5	2,7630	0,9299	7,4100	4,3263	2,4644	7,0600	56,58	165,03	-4,72
6	2,3391	1,3908	9,9600	4,3263	2,4644	7,0600	84,95	77,19	-29,12

According to the result of the validation experiments of Ttitanium alloy and mathematical models, it was seen that the error margin is in agreement for experiment results in the case of surface roughness. The same fit was far a little for MRR and incompatible for EWR.

According to observation of Inconel 718 test results which were obtained from mathematical models, it has seen that the error margin were low for each output parameter. The Ø400µm and Ø300µm experiment results had low error margin also. The experiment results which were carried out with Ø500µm, estimately half times more than predicted results for each parameter.

Table 5.9 Validation experiment's parameters of Inconel 718

Exp. No	Machining Parameters				MRR (mg/min)	EWR(mg/min)	R_a(µm)
	I(A)	T_{on}(µs)	T_{off}(µs)	D(µm)			
1	8.8	44	26	500	10,6225	2,655625	2,925
2	8.8	44	26	500	11,61409	3,164687	3,66
3	8.2	35	20	400	11,30261	3,607214	4,42
4	8.2	35	20	400	11,48031	3,685039	4,47
5	8.2	44	20	300	5,529709	2,020471	5,355
6	8.2	44	20	300	3,921358	1,646002	3,865

Table 5.10 Comparison of the validation experiments and mathematical results of Inconel 718

	Experimental			Mathematical			Error (%)		
Exp. No	MRR (mg/min)	EWR (mg/min)	R_a(µm)	MRR (mg/min)	EWR (mg/min)	R_a(µm)	MRR	EWR	R_a
1	10,6225	2,6556	2,925	17,4069	4,3616	1,7841	63,87	64,24	-39,01
2	11,6141	3,1647	3,660	17,4069	4,3616	1,7841	49,88	37,82	-51,25
3	11,3026	3,6072	4,420	12,6762	3,4238	4,1756	12,15	-5,08	-5,53
4	11,4803	3,6850	4,470	12,6762	3,4238	4,1756	10,42	-7,09	-6,59
5	5,5297	2,0205	5,355	3,3790	1,6418	3,0424	-38,89	-18,74	-43,19
6	3,9214	1,6460	3,865	3,3790	1,6418	3,0424	-13,83	-0,26	-21,28

5.3 Surface Observation

Inner surface of holes which were obtained as a result of the drilling process on both materials, were examined. This examination was performed with SEM imaging system. Result of Titanium alloy (experiment 8) test were seen at Figure 5.55 as result of drilling process. Also cracks can be seen on the side surface of the same hole (Figure 5.56). At the inner surface of the Inconel 718, experiment 8 of Ni-Ø500µm, cracks were found as shown in Figure 5.57 also. When the side surface of the same test piece was examined, there was no evidence for crack formation. On the other hand, as a result of Inconel 718 experiment number 9, cracks were occurred on the side surfaces as shown in Figure 5.58.

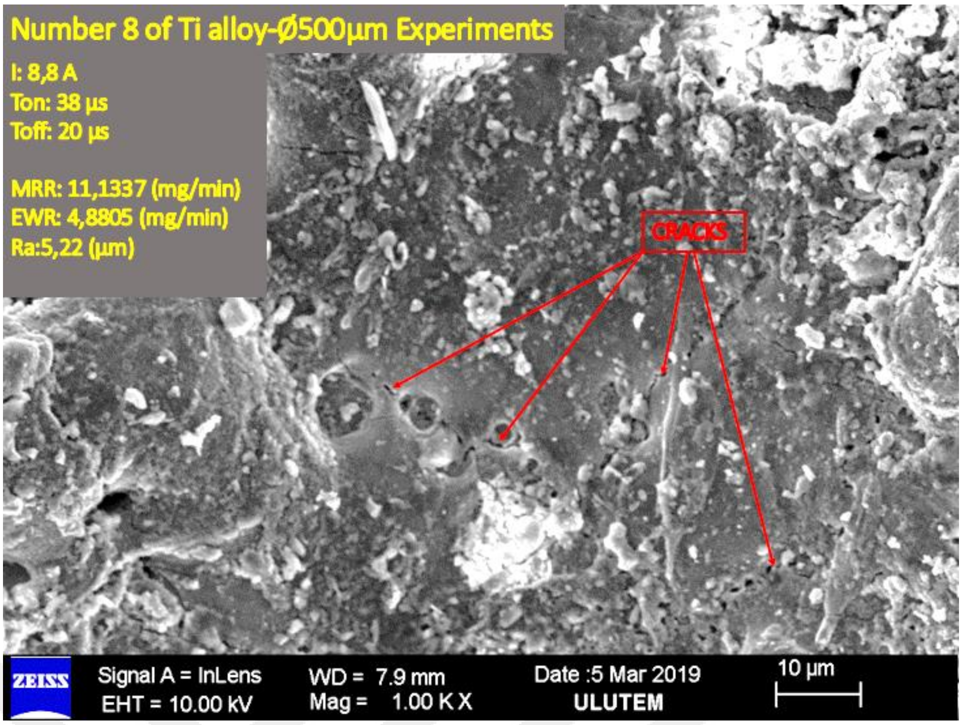

Figure 5.55 Crack appearance on SEM image, number 8 of Ti-Ø500µm experiments

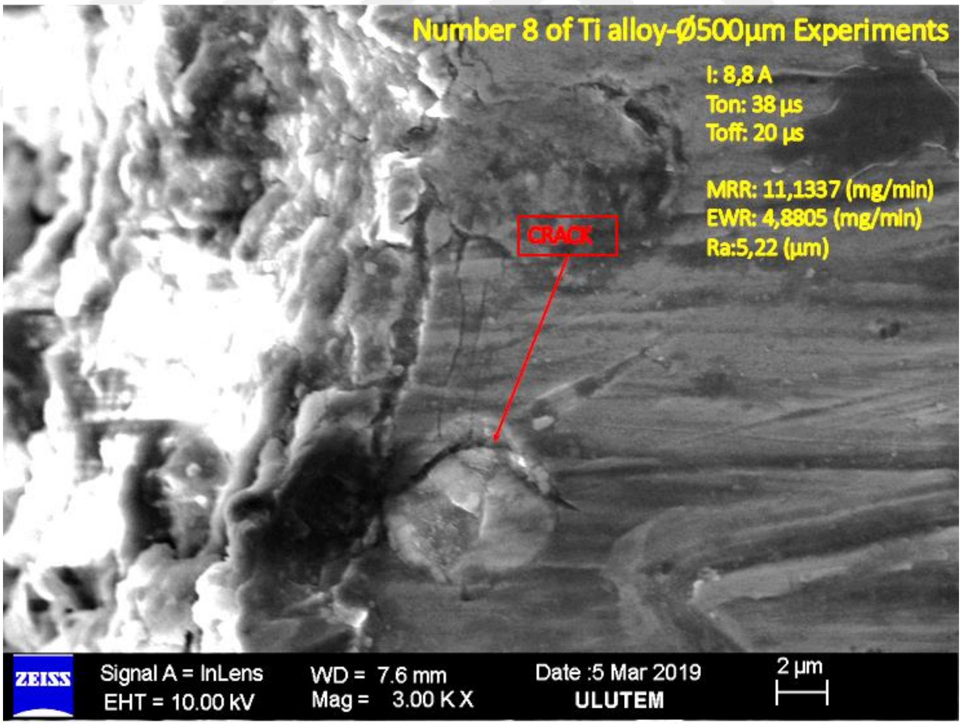

Figure 5. 56 Crack appearance on SEM image, number 8 of Ti-Ø500µm experiments

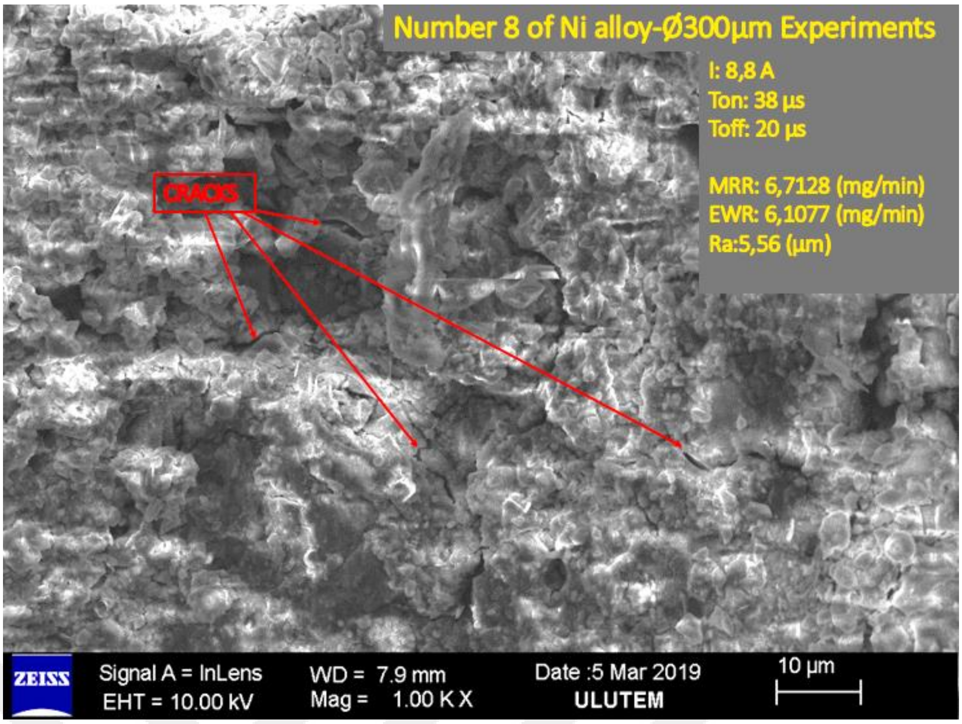

Figure 5.57 Crack appearance on SEM image, number 8 of Ni-Ø300µm experiments

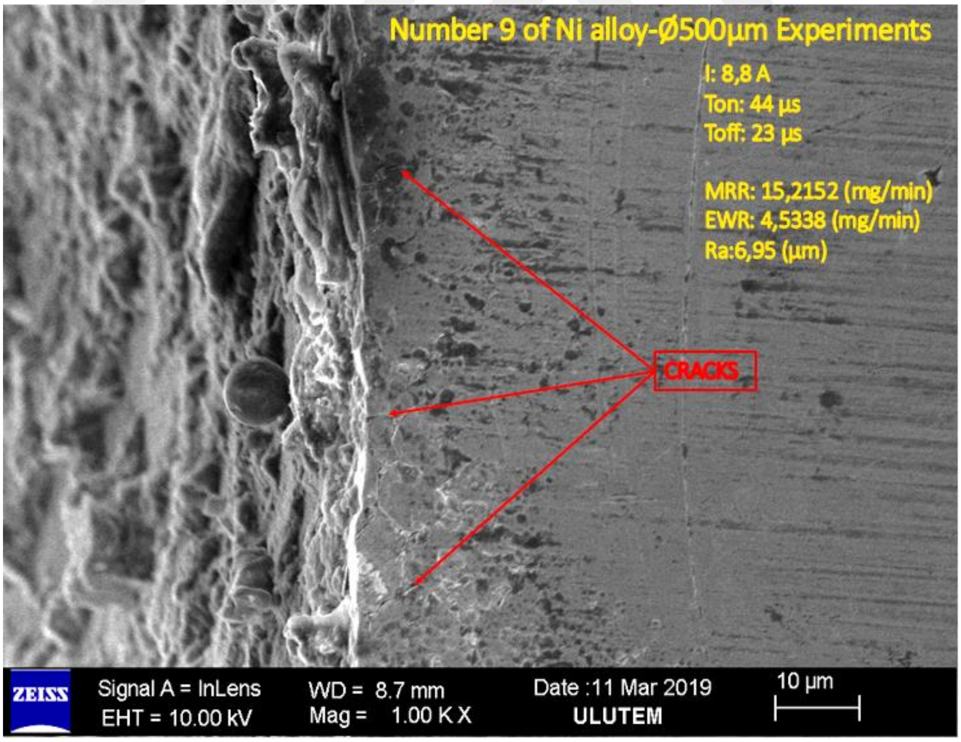

Figure 5.58 Crack appearance on SEM image, number 9 of Ni-Ø500µm experiments

CHAPTER VI

CONCLUSIONS

In this study, Micro-Hole EDM experiments which were designed with the Taguchi method was investigated. Output parameter's reliability has been proven with analysis of variance. R_a, MRR and EWR were chosen as experiment responses. Input parameters were selected as discharge current, pulse on time, pulse off time respectively. In order to conduct the tests accurately and precisely, the experiment design was prepared with Taguchi method. Experiments were carried out by regression analysis, which is a statistical method. Output parameters were recorded using measurement tools. Minitab was used during the studies.

Modeling and optimisation of the EDM process has been a part of this study. To do that, the relationship between EDM parameters and optimization tool was created by generating mathematical models. Optimization studies were applied to all diameters and the results were confirmed by validation experiments. Result of validation experiments, it has been shown that mathematical models can be used to calculate EDM drilling parameters. Some models should be reconstructed and confirmed by additional experimental studies. When the analysis results were examined, the following results can be achieved.

- This study have been carried out with Ø300/400/500µm single-hole brass electrode on Titanium and Nickel alloys. Result of experiments showed that the lower discharge currents ($I < 4A$) is not sufficient to evaporate the molten material properly due to less heat energy and result was very low MRR (less than 4 mg/min). Increment of Discharge current and pulse on time improved the melting and evaporation rate, so that MRR increased. Higher discharge currents values are caused very high electrode wear and lowest surface roughness according to other current parameters for Titanium alloy.

- Even though minimal pulse off time was required to increase MRR, a sufficient amount of pulse off time is necessary to remove the molten metal by the deionized water.
- Logical response function were designed by regression analysis and analyzed with ANOVA. The experiment results were proved as reliable according to ANOVA. Ti alloy-Ø500/400/300µm experiment results have been 0,9643, 0,9827 and 0,9201 r-sq respectively. Inconel 718-Ø500/400/300µm experiment results have been 0,9288, 0,8995, 0,7966 R-sq. The processed surfaces were examined by SEM and crater formation was observed on both kind of material's surfaces under high current parameter conditions.

REFERENCES

[1] Habib, S. (2009). Study of the parameters in electrical discharge machining through response surface methodology approach, *Applied Mathematical Modelling - Appl Math Model*. **33**, 4397-4407.

[2] Puranik, M., Joshi, S. (2008). Analysis of accuracy of high-aspect-ratio holes generated using micro-electric discharge machining drilling, *Proceedings of The Institution of Mechanical Engineers Part B-journal of Engineering Manufacture - Proc Inst Mech Eng B-J Eng Ma*. **222**, 1453-1464.

[3] Tosun, N., Çogun, C., Tosun, G. (2004). A study on kerf and material removal rate in wire electrical discharge machining based on Taguchi method, *Journal of Materials Processing Technology*. **152**, 316-322.

[4] Kumagai, S., Sato, N., Takeda, K. (2007). Operation parameter optimization for fabrication of a narrow, deep hole in metal by electrical discharge machining using a dielectric-encased wire electrode, *Journal of Materials Processing Technology - J Mater Process Technol*. **189**, 310-315.

[5] Debnath, S., Rai, R., Sastry, G. (2018). A Study of multiple regression analysis on die sinking EDM machining of Ex-Situ developed Al-4.5cu-SiC composite, *Materials today: proceedings*. **5**.

[6] Meena, V., Azad, M. (2012). Grey relational analysis of micro-EDM machining of Ti-6Al-4V alloy, *Materials and Manufacturing Processes - Mater Manuf Process*. **27**, 973-977.

[7] Eyercioglu, O., V. Cakir, M., Göv, K. (2013). Influence of machining parameters on the surface integrity in small-hole electrical discharge machining, *Proceedings of the Institution of Mechanical Engineers, Part B: Journal of Engineering Manufacture*. **228**, 51-61.

[8] Bellotti, M., Qian, J., Reynaerts, D. (2018). Enhancement of the micro-EDM process for drilling through-holes, p. 610-615.

[9] Yilmaz, O., Bozdana, A. T., Okka, M., Filiz, I. (2010). An intelligent and automated system for EDM hole drilling of super alloys, *IET Conference Publications*. **2010**, 95-99.

[10] Göv, K. (2017). Influence of the coolant on performance of electro Discharge hole drilling, *Journal of Polytechnic*. **20**, 191.

[11] Liu, N.-M., Chiang, K.-T., Horng, J.-T., Chen, C.-C. (2010). Modeling and analysis of the edge disintegration in the EDM drilling cobalt-bonded tungsten carbide, *The International Journal of Advanced Manufacturing Technology*. **51**, 587-598.

[12] Ekmekci, B., Sayar, A., Opoz, T., Erden, A. (2009). Geometry and surface damage in micro electrical discharge machining of micro-holes, *Journal of Micromechanics and Microengineering*. **19**, 105030.

[13] Puri, A., Bhattacharyya, B. (2005). Modeling and analysis of white layer depth in a wire-cut EDM process through response surface methodology, *International Journal of Advanced Manufacturing Technology*. **25**, 301-307.

[14] Göv, K. (2017). Experimental investigation of the effects of electrodes on EDM hole drilling process, *Journal of Polytechnic*. **20**, 100.

[15] Göv, K. (2016). Investigation of the effects of the dissolved oxygen in the coolant on the hole geometries drilled by electro erosion, *International Journal of Advanced Manufacturing Technology*. **31**, 231-239.

[16] Göv, K. (2017). The effects of the dielectric liquid temperature on the hole geometries drilled by electro erosion, *The International Journal of Advanced Manufacturing Technology*. **92**.

[17] Valaki, J., Rathod, P., Sankhavara, C. D. (2016). Investigations on technical feasibility of Jatropha curcas oil based bio dielectric fluid for sustainable electric discharge machining (EDM), *Journal of Manufacturing Processes*. **22**, 151-160.

[18] Fonseca, J., Marafona, J. (2014). The effect of deionisation time on the electrical discharge machining performance, *The International Journal of Advanced Manufacturing Technology*. **71**.

[19] Ishida, T., Takeuchi, Y. (2002). L-Shaped curved hole creation by means of electrical discharge machining and an electrode curved motion Generator, *International Journal of Advanced Manufacturing Technology*. **19**, 260-265.

[20] Okada, A., Yamaguchi, A., Ota, K. (2017). Improvement of curved hole EDM drilling performance using suspended ball electrode by workpiece vibration, *CIRP Annals - Manufacturing Technology*. **66**.

[21] Maradia, U., Benavoli, A., Boccadoro, M., Bonesana, C., Klyuev, M., Zaffalon, M., Gambardella, L., Wegener, K. (2018). EDM drilling optimisation using stochastic techniques, *Procedia CIRP*. **67**, 350-355.

[22] Kumar, P., Parkash, R. (2016). Experimental investigation and optimization of EDM process parameters for machining of aluminum boron carbide (Al–B 4 C) composite, *Machining Science and Technology*. **20**, 330-348.

[23] Duraisamy, P., Devaraju, A., Manikandan, N., Balasubramanian, K., D, A. (2019). Experimental investigation and optimization of process parameters in EDM of aluminium metal matrix composites, *Materials Today: Proceedings*.

[24] Bellotti, M., Qian, J., Reynaerts, D. (2019). Breakthrough phenomena in drilling micro holes by EDM, *International Journal of Machine Tools and Manufacture*. 103436.

[25] Sapkal, S., Jagtap, P. (2018). Optimization of micro EDM drilling process parameters for titanium alloy by rotating electrode, *Procedia Manufacturing*. **20**, 119-126.

[26] Natsu, W., Maeda, H. (2018). realization of high-speed micro EDM for high-aspect-ratio micro hole with mist nozzle, *Procedia CIRP*. **68**, 575-577.

[27] Perveen, A., Jahan, M. (2018). Modeling and optimization of crater size generated during micro- EDM of Ti alloy using Response surface method, *Materials Today: Proceedings*. **5**, 18307-18314.

[28] Skrabalak, G. (2018). Influence of electrode tool length on the micro EDM drilling performance, *Procedia CIRP*. **68**, 594-598.

[29] Aharwal, K. R., Sitaram, Krishna, C. M. (2018). Optimization of material removal rate and surface roughness in EDM machining of metal matrix composite using genetic algorithm, *Materials Today: Proceedings*. **5**, 5391-5397.

[30] Kliuev, M., Baumgart, C., Büttner, H., Wegener, K. (2018). Flushing velocity observations and analysis during EDM drilling, *Procedia CIRP*. **77**, 590-593.

[31] M, D., Potnuru, S. r., Valli, P. (2018). Optimization of EDM process parameters by using heuristic approach, *Materials Today: Proceedings*. **5**, 27036-27042.

[32] Bhosle, R., Sharma, S. B. (2017). Multi-performance optimization of micro-EDM drilling process of Inconel 600 alloy, *Materials Today: Proceedings*. **4**, 1988-1997.

[33] Tripathy, S., Tripathy, D. K. (2017). Surface characterization and multi-response optimization of EDM process parameters using powder mixed dielectric, *Materials Today: Proceedings*. **4**, 2058-2067.

[34] Begum, A., Reddy, D. (2017). Effect of polarity on the machining characteristics and surface generation in EDM, *Materials Today: Proceedings*. **4**, 7674-7679.

[35] Kumar, R., Thakur, S., Pandey, D. A. (2017). Modelling and optimization of hole circularity and hole dilation in electrical discharge drilling, *Materials Today: Proceedings*. **4**, 8706-8716.

[36] Surya, V., Kumar, K. M., R, K., Gonchikar, U., Ravindra, H. V. (2017). Prediction of machining characteristics using artificial neural network in wire EDM of Al7075 based In-situ composite, *Materials Today: Proceedings*. **4**, 203-212.

[37] Janardhanan, J., Ramnath, V., Elanchezhian, C., Akilesh, S. (2017). Optimization of process parameters in Electro-chemical machining (ECM) of D3 die steels using Taguchi technique, *Materials Today: Proceedings*. **4**, 7884-7891.

[38] Mohanty, C., Mahapatra, S., Singh, D. M. (2016). An intelligent approach to optimize the EDM process parameters using utility concept and QPSO algorithm, *Engineering Science and Technology, an International Journal*. **20**.

[39] Rahul, Datta, S. (2019). Electrical discharge machining performance of deep cryogenically treated Inconel 825 superalloy: emphasis on surface integrity, *Materials Characterization*. **8**, 212–225.

[40] Uhlmann, E., Schimmelpfennig, T.-M., Perfilov, I., Streckenbach, J., Schweitzer, L. (2016). Comparative analysis of dry-EDM and conventional EDM for the manufacturing of micro holes in Si3N4-TiN, *Procedia CIRP*. **42**, 173-178.

[41] Uhlmann, E., Perfilov, I., Yabroudi, S., Schweitzer, L., Polte, M. (2018). Electro-discharge drilling with MP-based carbon fibre electrode, in euspen 18th International Conference & Exhibition: Venice, Italy.

[42] Risto, M., Haas, R., Munz, M. (2016). Optimization of the EDM drilling process to increase the productivity and geometrical accuracy, *Procedia CIRP*. **42**, 537-542.

[43] Kliuev, M., Boccadoro, M., Perez, R., Bó, W., Stirnimann, J., Kuster, F., Wegener, K. (2016). EDM drilling and shaping of cooling holes in inconel 718 turbine blades, *Procedia CIRP*. **42**, 322-327.

[44] Antar, M., Chantzis, D., Marimuthu, S., Hayward, P. (2016). High speed EDM and laser drilling of aerospace alloys, *Procedia CIRP*. **42**, 526-531.

[45] Fu, X., Gao, L., Zhang, Q., Liu, Q. (2016). Surface roughness research of piezoelectric self-adaptive micro-EDM, *Procedia CIRP*. **42**, 563-568.

[46] Lin, Y.-C., Hung, J.-C., Chow, H.-M., Wang, A. C., Chen, J.-T. (2016). Machining characteristics of a hybrid process of EDM in gas combined with ultrasonic vibration and AJM, *Procedia CIRP*. **42**, 167-172.

[47] Che, J., Zhou, T., Zhu, X., Kong, W., Wang, Z., Xie, X. (2016). Experimental study on horizontal ultrasonic electrical discharge machining, *Journal of Materials Processing Technology*. **231**.

[48] Teimouri, R., Baseri, H. (2014). Optimization of magnetic field assisted EDM using the continuous ACO algorithm, *Applied Soft Computing*. **14**, 381–389.

[49] D'Urso, G., Merla, C. (2014). Workpiece and electrode influence on micro-EDM drilling performance, *Precision Engineering*. **38**.

[50] Plaza, S., Sanchez, J., Perez, E., Gil, R., Izquierdo, B., Ortega, N., Pombo, I. (2014). Experimental study on micro EDM-drilling of Ti6Al4V using helical electrode, *Precision Engineering*. **38**.

[51] Jameson, E. C. (2001). *Electrical discharge machining. Society of Manufacturing Engineers*. Dearborn, Michigan.

[52] Sommer, C., Sommer, S., Sommer, P. (2005). *Complete EDM Handbook*. www.reliableedm.com

[53] Youssef, H. A., El-Hofy, H. (2008). *Machining technology: Machine tools and operations*. CRC Press, Taylor & Francis Group, 672.

[54] Çakır, M. V. (2014). Evaluation of multi-stage electro discharge machining (EDM) parameters, in Mechanical Engineering: University of Gaziantep.

[55] Maji, K., Pratihar, D. (2010). Forward and reverse mappings of electrical discharge machining process using adaptive network-based fuzzy inference system, *Expert Syst. Appl.* **37**, 8566-8574.

[56] Mandal, D., Pal, S., Saha, P. (2007). Modeling of electrical discharge machining process using back propagation neural network and multi-objective optimization using non-dominating sorting genetic algorithm-II, *Journal of Materials Processing Technology*. **186**, 154-162.

[57] Yilmaz, O., Eyercioglu, O., Gindy, N. (2006). A user-friendly fuzzy-based system for the selection of electro discharge machining process parameters, *Journal of Materials Processing Technology*. **172**, 363-371.

[58] Amorim, F., Weingaertner, W. (2007). The Behavior of graphite and copper electrodes on the finish die-sinking electrical discharge machining (EDM) of AISI P20 tool steel, *Journal of The Brazilian Society of Mechanical Sciences and Engineering - J Braz Soc Mech Sci Eng*. **29**.

[59] Haron, C., Ghani, J., Burhanuddin, Y., Seong, Y., Swee, C. (2008). Copper and graphite electrodes performance in electrical-discharge machining of XW42 tool steel, *Journal of Materials Processing Technology - J Mater Process Technol*. **201**, 570-573.

[60] Armstrong, N. A. (2006). *Pharmaceutical experimental design and interpretation*. New York: CRC Press, Taylor & Francis Group.

[61] Roy, R. K. (2001). *Design of experiments using the Taguchi approach*. New York: John Willey & Sons, Inc.

[62] Okka, M. A. (2011). An experimental investigation of electrical discharge machining (EDM) fast hole drilling of Inconel 718 and Ti6Al4V, in Mechanical Engineering: University of Gaziantep.

[63] Kuppan, P., Rajadurai, A., Narayanan, S. (2008). Influence of EDM process parameters in deep hole drilling of Inconel 718, *International Journal of Advanced Manufacturing Technology*. **38**, 74-84.

[64] Soni, J. S., Chakraverti. (1993). Surface characteristics of titanium with rotary EDM, *Bull. Mater. Sci.* **16**(3), 213-227.

APPENDICES

Appendix A: ANOVA Tests of Ti-6Al-4V Experiments

Appendix B: ANOVA Tests of Inconel 718 Experiments

Appendix A

Table A.1 MRR (mg/min) for Ø500μm

Analysis of Variance					
Source	DF	Adj SS	Adj MS	F-Value	P-Value
Regression	3	148,891	49,63	44,98	0
I	1	148,134	148,134	134,25	0
T_{on}	1	0,001	0,001	0	0,974
T_{off}	1	0,756	0,756	0,69	0,445
Error	5	5,517	1,103		
Total	8	154,408			

Model Summary

S	R-sq	R-sq(adj)
1,05042	96,43%	94,28%

Table A.2 EWR (mg/min) for Ø500μm

Analysis of Variance					
Source	DF	Adj SS	Adj MS	F-Value	P-Value
Regression	3	34,8277	11,6092	94,42	0
I	1	33,2255	33,2255	270,23	0
T_{on}	1	0,8869	0,8869	7,21	0,044
T_{off}	1	0,7153	0,7153	5,82	0,061
Error	5	0,6148	0,123		
Total	8	35,4425			

Model Summary

S	R-sq	R-sq(adj)
0,350644	98,27%	97,22%

Table A.3 R_a (mg/min) for Ø500μm

Analysis of Variance					
Source	DF	Adj SS	Adj MS	F-Value	P-Value
Regression	3	154,432	51,477	19,18	0,004
I	1	153,111	153,111	57,06	0,001
T_{on}	1	0,627	0,627	0,23	0,649
T_{off}	1	0,694	0,694	0,26	0,633
Error	5	13,418	2,684		
Total	8	167,85			

Model Summary

S	R-sq	R-sq(adj)
1,63814	92,01%	87,21%

Table A.4 MRR (mg/min) for Ø400µm

Analysis of Variance					
Source	DF	Adj SS	Adj MS	F-Value	P-Value
Regression	6	60,1105	10,0184	17,9	0,054
I	2	56,049	28,0245	50,09	0,02
T_{on}	2	3,3296	1,6648	2,98	0,252
T_{off}	2	0,7319	0,366	0,65	0,605
Error	2	1,1191	0,5595		
Total	8	61,2296			

Model Summary

S	R-sq	R-sq(adj)
0,748022	98,17%	92,69%

Table A.5 EWR (mg/min) for Ø400µm

Analysis of Variance					
Source	DF	Adj SS	Adj MS	F-Value	P-Value
Regression	6	14,9222	2,487	24,22	0,04
I	2	13,433	6,7165	65,41	0,015
T_{on}	2	1,2198	0,6099	5,94	0,144
T_{off}	2	0,2694	0,1347	1,31	0,433
Error	2	0,2054	0,1027		
Total	8	15,1276			

Model Summary

S	R-sq	R-sq(adj)
0,320434	98,64%	94,57%

Table A.6 R_a (mg/min) for Ø400µm

Analysis of Variance					
Source	DF	Adj SS	Adj MS	F-Value	P-Value
Regression	6	134,349	22,3916	2,5	0,313
I	2	119,847	59,9234	6,69	0,13
T_{on}	2	0,087	0,0435	0	0,995
T_{off}	2	14,416	7,2078	0,81	0,554
Error	2	17,907	8,9534		
Total	8	152,256			

Model Summary

S	R-sq	R-sq(adj)
2,99222	88,24%	52,96%

Table A.7 MRR (mg/min) for Ø300μm

Analysis of Variance					
Source	DF	Adj SS	Adj MS	F-Value	P-Value
Regression	3	17,9005	5,9668	79,4	0
I	1	17,7959	17,7959	236,79	0
T_{on}	1	0,096	0,096	1,28	0,31
T_{off}	1	0,0087	0,0087	0,12	0,747
Error	5	0,3758	0,0752		
Total	8	18,2763			

Model Summary

S	R-sq	R-sq(adj)
0,274142	97,94%	96,71%

Table A.8 EWR (mg/min) for Ø300μm

Analysis of Variance					
Source	DF	Adj SS	Adj MS	F-Value	P-Value
Regression	6	3,2253	0,53755	3,78	0,224
I	2	2,7826	1,39131	9,78	0,093
T_{on}	2	0,2556	0,12779	0,9	0,527
T_{off}	2	0,1871	0,09354	0,66	0,603
Error	2	0,2845	0,14223		
Total	8	3,5097			

Model Summary

S	R-sq	R-sq(adj)
0,377135	91,90%	67,58%

Table A.9 R_a (mg/min) for Ø300μm

Analysis of Variance					
Source	DF	Adj SS	Adj MS	F-Value	P-Value
Regression	3	271,044	90,348	17,8	0,004
I	1	266,699	266,699	52,55	0,001
T_{on}	1	2,485	2,485	0,49	0,515
T_{off}	1	1,859	1,859	0,37	0,571
Error	5	25,375	5,075		
Total	8	296,418			

Model Summary

S	R-sq	R-sq(adj)
2,25276	91,44%	86,30%

Appendix B

Table B.1 MRR (mg/min) for Ø500µm

Analysis of Variance					
Source	DF	Adj SS	Adj MS	F-Value	P-Value
Regression	3	153,79	51,263	21,74	0,003
I	1	81,77	81,775	34,68	0,002
T_{on}	1	57,62	57,622	24,43	0,004
T_{off}	1	14,39	14,393	6,1	0,057
Error	5	11,79	2,358		
Total	8	165,58			

Model Summary

S	R-sq	R-sq(adj)
1,53567	92,88%	88,61%

Table B.2 EWR (mg/min) for Ø500µm

Analysis of Variance					
Source	DF	Adj SS	Adj MS	F-Value	P-Value
Regression	3	19,6143	6,5381	14,91	0,006
I	1	13,0824	13,0824	29,84	0,003
T_{on}	1	6,3939	6,3939	14,59	0,012
T_{off}	1	0,138	0,138	0,31	0,599
Error	5	2,1918	0,4384		
Total	8	21,8061			

Model Summary

S	R-sq	R-sq(adj)
0,662087	89,95%	83,92%

Table B.3 R_a (mg/min) for Ø500µm

Analysis of Variance					
Source	DF	Adj SS	Adj MS	F-Value	P-Value
Regression	3	66,346	22,115	6,53	0,035
I	1	55,34	55,34	16,34	0,01
T_{on}	1	2,124	2,124	0,63	0,464
T_{off}	1	8,882	8,882	2,62	0,166
Error	5	16,937	3,387		
Total	8	83,282			

Model Summary

S	R-sq	R-sq(adj)
1,84047	79,66%	67,46%

Table B.4 MRR (mg/min) for Ø400μm

Analysis of Variance					
Source	DF	Adj SS	Adj MS	F-Value	P-Value
Regression	3	122,787	40,929	57,87	0
I	1	111,24	111,24	157,3	0
T_{on}	1	11,476	11,476	16,23	0,01
T_{off}	1	0,071	0,071	0,1	0,764
Error	5	3,536	0,707		
Total	8	126,323			

Model Summary		
S	R-sq	R-sq(adj)
0,840953	97,20%	95,52%

Table B.5 EWR (mg/min) for Ø400μm

Analysis of Variance					
Source	DF	Adj SS	Adj MS	F-Value	P-Value
Regression	3	14,9917	4,9972	6,74	0,033
I	1	14,9891	14,9891	20,23	0,006
T_{on}	1	0,0017	0,0017	0	0,964
T_{off}	1	0,0009	0,0009	0	0,974
Error	5	3,7056	0,7411		
Total	8	18,6972			

Model Summary		
S	R-sq	R-sq(adj)
0,860881	80,18%	68,29%

Table B.6 R_a (mg/min) for Ø400μm

Analysis of Variance					
Source	DF	Adj SS	Adj MS	F-Value	P-Value
Regression	3	27,0125	9,0042	6,07	0,04
I	1	25,4612	25,4612	17,16	0,009
T_{on}	1	1,5246	1,5246	1,03	0,357
T_{off}	1	0,0267	0,0267	0,02	0,899
Error	5	7,4169	1,4834		
Total	8	34,4294			

Model Summary		
S	R-sq	R-sq(adj)
1,21794	78,46%	65,53%

Table B.7 MRR (mg/min) for Ø300μm

Analysis of Variance					
Source	DF	Adj SS	Adj MS	F-Value	P-Value
Regression	3	33,1869	11,0623	13,16	0,008
I	1	30,2457	30,2457	35,97	0,002
T_{on}	1	1,9668	1,9668	2,34	0,187
T_{off}	1	0,9744	0,9744	1,16	0,331
Error	5	4,2045	0,8409		
Total	8	37,3914			

Model Summary		
S	R-sq	R-sq(adj)
0,917005	88,76%	82,01%

Table B.8 EWR (mg/min) for Ø300μm

Analysis of Variance					
Source	DF	Adj SS	Adj MS	F-Value	P-Value
Regression	3	19,7444	6,5815	5,96	0,042
I	1	19,4632	19,4632	17,63	0,009
T_{on}	1	0,2047	0,2047	0,19	0,685
T_{off}	1	0,0765	0,0765	0,07	0,803
Error	5	5,5206	1,1041		
Total	8	25,265			

Model Summary		
S	R-sq	R-sq(adj)
1,05077	78,15%	65,04%

Table B.9 R_a (mg/min) for Ø300μm

Analysis of Variance					
Source	DF	Adj SS	Adj MS	F-Value	P-Value
Regression	3	21,839	7,2797	5,48	0,049
I	1	21,8389	21,8389	16,44	0,01
T_{on}	1	0,0001	0,0001	0	0,994
T_{off}	1	0	0	0	0,997
Error	5	6,64	1,328		
Total	8	28,4791			

Model Summary		
S	R-sq	R-sq(adj)
1,15239	76,68%	62,70%